

***A Detail investigation to observe the effect of zinc oxide
and Silver nanoparticles in biological system.***

Thesis submitted

By

BARNALI ASHE (607BM004)

In partial fulfillment for the award of the degree of Master of
Technology (Research)

In

Biotechnology and Medical Engineering



Department of Biotechnology & Medical Engineering

National Institute Of Technology

Rourkela-769008, Orissa, India

January 2011

***A Detail investigation to observe the effect of zinc oxide
and Silver nanoparticles in biological system.***

Thesis submitted

By

BARNALI ASHE (607BM004)

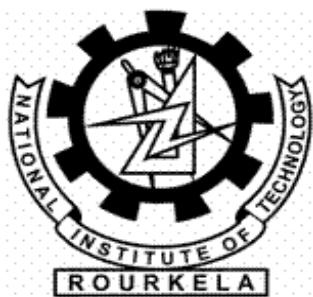
In partial fulfillment for the award of the degree of Master of
Technology (Research)

In

Biotechnology and Medical Engineering

Under the Guidance of

Dr. Subhankar Paul

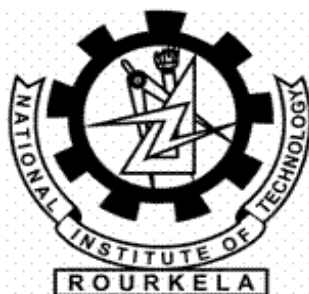


Department of Biotechnology & Medical Engineering

National Institute Of Technology Rourkela-769008, Orissa, India

CERTIFICATE

Date-13.01.2011



This is to certify that the thesis entitled “*A Detail investigation to observe the effect of zinc oxide and Silver nanoparticles in biological system*” is submitted by **Barnali Ashe**, (Roll NO- **607bm004**) to this Institute in partial fulfillment of the requirement for the award of the degree of Master of Technology by Research in **Department of Biotechnology and Medical Engineering**, is a bonified record of the work carried out under my supervision and guidance. It is further certified that no part of this thesis is submitted for the award of any degree.

Dr. Subhankar Paul

ACKNOWLEDGEMENT

In pursuit of this academic endeavor I feel that I have been especially fortunate as inspiration, guidance, direction, co-operation, love and care all came in my way in abundance and it seems almost an impossible task for me to acknowledge the same in adequate terms.

I express my sincere thanks to my supervisor, **Dr. Subhankar Paul, Associate Profesor**, Department of 'Biotechnology and Medical Engineering', NIT Rourkela, for his esteemed supervision, incessant support, inspiration and constructive criticism throughout my research work.

I extend my sincere thanks to **Prof Krishna Pramanik**, Professor Department of Biotechnology and Medical Engineering, N.I.T. Rourkela for giving the kind permission and providing me the necessary laboratory facilities to carry out this work.

I accord my thanks to **Dr. Amit Biswas**, Department of Biotechnology and Medical Engineering, NIT Rourkela, for providing me with all necessary administrative facilities during the research work.

I am also thankful to **Prof S.K. Prathiar** and **Prof J. Bera**, Department of Ceramic Engineering for their kind help in XRD analysis and DLS particle size analysis and I also sincerely thank to Metallurgical and Material Engineering department for assisting in SEM analysis during my research work.

I would like to take the opportunity to thank all friends and lab mates Devendra Bramah Singh, Smurti rekha Das, Ganesh sahu, Navneet kumar Dubey, Sourabh choudhry, Tulsi swain, Rajdeep Kaur, Priyadarshini Pattanayak, Anjul, Bhanuprakash and Sailendra Mohanta for their help and motivation. I will relish your memories for years to come.

Finally, I would also express my sincere gratitude to my parents, brother and beloved husband for their encouragement and support throughout, which always inspired me.

I would also express my sincere thanks to laboratory Members of Department of Biotechnology and Medical Engineering, N.I.T. Rourkela.

BARNALI ASHE.

ACKNOWLEDGEMENT

In pursuit of this academic endeavor I feel that I have been especially fortunate as inspiration, guidance, direction, co-operation, love and care all came in my way in abundance and it seems almost an impossible task for me to acknowledge the same in adequate terms.

I express my sincere thanks to my supervisor, **Dr. Subhankar Paul, Associate Profesor**, Department of 'Biotechnology and Medical Engineering', NIT Rourkela, for his esteemed supervision, incessant support, inspiration and constructive criticism throughout my research work.

I extend my sincere thanks to **Prof Krishna Pramanik**, Professor Department of Biotechnology and Medical Engineering, N.I.T. Rourkela for giving the kind permission and providing me the necessary laboratory facilities to carry out this work.

I accord my thanks to **Dr. Amit Biswas**, Department of Biotechnology and Medical Engineering, NIT Rourkela, for providing me with all necessary administrative facilities during the research work.

I am also thankful to **Prof S.K. Prathiar** and **Prof J. Bera**, Department of Ceramic Engineering for their kind help in XRD analysis and DLS particle size analysis and I also sincerely thank to Metallurgical and Material Engineering department for assisting in SEM analysis during my research work.

I would like to take the opportunity to thank all friends and lab mates Devendra Bramah Singh, Smurti rekha Das, Ganesh sahuo, Navneet kumar Dubey, Sourabh choudhry, Tulsi swain, Rajdeep Kaur, Priyadarshini Pattanayak, Anjul, Bhanuprakash and Sailendra Mohanta for their help and motivation. I will relish your memories for years to come.

Finally, I would also express my sincere gratitude to my parents, brother and beloved husband for their encouragement and support throughout, which always inspired me.

I would also express my sincere thanks to laboratory Members of Department of Biotechnology and Medical Engineering, N.I.T. Rourkela.

BARNALI ASHE.

ABSTRACT

In the present investigation, synthesis and characterization of Zinc Oxide (ZnO) and Silver nanoparticles (NP), and their application on pathogenic bacteria were investigated. ZnO NP were synthesized by chemical reduction method using starch as capping agent and silver NP was prepared by green synthesis process from AgNO₃ solution through the extract of *Citrus sinensis* (sweet lime). The detail characterization of the nanoparticles was carried out using UV-Vis spectroscopy, Dynamic Light Scattering (DLS) particle size analysis, Scanning Electron Microscopy (SEM), X-Ray Diffraction (XRD) analysis and Thermogravimetric (TGA) analysis. From Dynamic Light Scattering (DLS) particle size and SEM image analysis, the average particle size was found to be 90 nm and 50 nm, for ZnO and silver nanoparticles, respectively. From the analysis of XRD pattern, UV-VIS spectroscopy and TGA, the formation of nanoparticles was confirmed. Antibacterial assay of synthesized ZnO and silver NP was carried out both in liquid and solid growth medium against four pathogens (*Escherichia coli*, *Bacillus subtilis*, *Pseudomonas aeruginosa*, and *streptococcus pneumonia*). The bacterial growth was monitored by measuring the optical density (OD) of culture solution and estimation of colony forming units (CFU) on solid medium. The effect of NP on the level of gene expression in *E.coli* was also examined. When NP was administered in the liquid *E.coli* culture, considerable enhancement of the enzymatic activity of expressed β -glucosidase was observed. Further the physical interaction between bovine α -lactalbumin protein and NP was monitored by DLS particle size analyzer, tryptophan fluorescence and circular dichroism spectroscopy. From DLS particle size analyzer, the protein was found to form stable conjugate with NP. When the interaction was monitored by tryptophan fluorescence spectroscopy, a drastic conformational change of the protein was observed. The

interaction was also monitored by circular dichroism spectroscopy. It revealed that on binding, nanoparticles caused substantial change in the secondary structure of the protein which indeed in complete agreement with tertiary conformational change monitored by fluorescence spectroscopy.

Key Words: Nanoparticles (ZnO and Silver), antimicrobial effect, β -glucosidase, α -lactalbumin , tryptophan fluorescence, circular dichroism spectroscopy protein-nanoparticles conjugate.

Table of Contents

CERTIFICATE

ACKNOWLEDGEMENT I-II

ABSTRACT III-IV

LIST OF FIGURES V-VII

LIST OF TABLES VIII

NOMENCLATURE IX

1. INTRODUCTION 1-7

1.1 Background 1

1.2 ZnO nanoparticles 2-4

1.3 Silver nanoparticles 4-5

1.4 β -glucosidase 6

1.5 Study on the interaction of protein and nanoparticles 6-7

2. REVIEW OF LITERATURE 8-28

2.1 History 8

2.2 Concept of nanoparticles 8-9

2.3 Application of nanoparticles 9-10

2.4 ZnO nanoparticles	10-15
2.4.1 Synthesis of ZnO nanoparticles	11
2.4.2 Application of ZnO	11-12
2.4.3 Antibacterial potential of ZnO	12-15
2.5 Silver nanoparticles	15-19
2.5.1 Synthesis of Ag nanoparticles	16-18
2.5.2 Biochemical synthesis of Ag nanoparticles	18-19
2.6 Application of Ag nanoparticles	19-21
2.6.1 Human health	19
2.6.2 Enviromental	20
2.6.3 Catalytic action	20
2.6.4 Antimicrobial	21
2.7 β -glucosidase	22-24
2.8 α lactolbumin	24-25
2.8.1 Importance of α lactolbumin	24-25
2.9 Study of protein nanoparticles interaction	25-27
2.10 Motivation	27
2.11 Objectives	28
 3. MATERIALS AND METHODS	 29-41
3.1 General	29

3.2 Chemicals	30
3.3 . Glassware and Apparatus	30
3.4 Synthesis of ZnO nanoparticles	30-31
3.5 Synthesis of silver nanoparticles	32-33
3.6 Characterization techniques	34-36
3.6.1 UV-Vis Spectroscopy	34
3.6.2 X-RAY Diffraction method	34-35
3.6.3 Scanning electron microscope (SEM)	35
3.6.4 DLS particle size analyzer	35
3.6.5 Thermo gravimetric analysis	36
3.7 Antibacterial test	36-38
3.7.1 Growth inhibition in liquid medium	36-37
3.7.2 Disc Diffusion Method	37-38
3.7.3 Colony forming unit Measurement	38
3.8 Effect of NP on <i>in vivo</i> gene expression level in <i>E.coli</i>	38-39

3.9 Formation of α -lactalbumin and silver nanoparticles complex	39
3.10 <i>In vitro</i> interaction of Ag nanoparticles and bovine α -lactalbumin	39-41
3.10.1 Tryptophan fluorescence emission spectra	39
3.10.2 Quenching studies of bovine α -lactalbumin	40
3.10.3 Far UV CD spectroscopy	40- 41
 4. RESULTS AND DISCUSSION	 42-73
 4.1 synthesis of ZnO and Silver Nanoparticles	 42-43
4.2 Characterization of ZnO and Ag nanoparticles	43-50
4.2.1 UV-Vis Spectroscopy	42-43
4.2.2 Analysis of X-RAY Diffraction pattern	44-45
4.2.3 Scanning electron microscope (SEM)	46-47
4.2.4 EDX analysis	46-47
4.2.5 .Analysis of DLS particle size analyzer	48-49
4.2.6 Thermo gravimetric analysis	50

4.3 Results of antibacterial assay of ZnO and Ag nanoparticles	51-59
4.4 Effect of NP in genetic expression level of β -glucosidase	59-61
4.5 Formation of conjugate between α -lactalbumin and ZnO	62-64
4.6 Formation of conjugate between α -lactalbumin and Ag	65-67
4.7 <i>In vitro</i> interaction of Ag nanoparticles and bovine α -lactalbumin	68-73
4.7.1 <i>Results of tryptophan fluorescence emission spectra</i>	68-69
4.7.2 <i>Analysis of Far-UV CD measurement</i>	70-73
5. CONCLUSION	74-76
6. REFERENCES	77-85

LIST OF FIGURES

Figure 1. Schematic diagram of synthesis of ZnO NP sample

Figure 2. Schematic diagram of synthesis of Ag NP sample

Figure 3. Synthesized ZnO NP powder by chemical reduction method

Figure 4. Digital photographs of (a) *Citrus sinensis* extract (b) 1 mM AgNO₃ without *citrus sinensis* extract (c) 1 mM AgNO₃ with sweet lime extract after 10 hrs of incubation.

Figure 5. UV-Vis spectra of the (a) ZnO synthesized by chemical reduction method and (b) Silver nanoparticles prepared with 0.5% of soluble starch and 1mM aqueous AgNO₃ solution with 10% *Citrus sinensis* extract.

Figure 6. (a) XRD patterns of ZnO nanoparticles (red) bulk ZnO (black) ZnO synthesized using 0.5% starch. The peaks assigned to diffractions from various planes are of hcp ZnO. (b) The silver nanoparticles synthesized by treating 10% *Citrus sinensis* extract with 1 mM aqueous AgNO₃ solution

Figure 7. SEM micrograph and EDX of ZnO and silver nanoparticles synthesized by chemical reduction method and green synthesis process, respectively.

Figure 8. Particle size distribution of (a) ZnO synthesized by chemical reduction method and (b) Silver nanoparticles synthesized by green synthesis process.

Figure 9. Thermo gravimetric analysis of bulk ZnO (red), nano-ZnO (blue) and soluble starch (black).

Figure 10. Images of antibacterial activities of discs of different concentration of ZnO.

Figure 11. Images of antibacterial activities of discs of different concentration of silver nanoparticles

Figure 12. Antimicrobial characterization by CFU as a function of ZnO and silver nanoparticles concentration on agar plates.

Figure 13. Digital photograph of number of *E. coli* colonies as a function of the concentration of silver nanoparticles in nutrient agar plate.

Figure 14. The effect of ZnO and silver nanoparticles on the growth of *E. Coli*.

Figure 15. The effect of β -glucosidase activity with ZnO nanoparticles treated with *E.coli* strain.

Figure 16. Activity of β -glucosidase activity with silver nanoparticles treated *E.coli* strain.

Figure 17. Conversion of PNPG to PNP and glucose

Figure 18. Formation of conjugate between α -lactalbumin and ZnO nanoparticles monitored by DLS particle size analyzer.

Figure 19. Formation of complex α -lac albumin and Ag NP was monitored by DLS.

Figure 20. Intrinsic fluorescence spectrum of 0.2mg/ml bovine α -lactalbumin in 20 mM sodium phosphate buffer, pH 7.0.

Figure 21. Emission fluorescence spectrum of (a) pure α -lactalbumin (0.2mg/ml), (b) α -lactalbumin-AgNP complex and (c) pure Ag nanoparticle (50 μ g/ml).

Figure 22. Emission fluorescence spectrum of pure (a) α -lactalbumin (0.2mg/ml) (b) pure protein in the presence of 200 mM acrylamide (c) Pure Ag nanoparticle (50 μ g/ml) , and (d) α -lactalbumin-AgNP complex, (e) α -lactalbumin-NP complex in presence of 200 mM acrylamide.

Figure 23. CD spectrum of (a) Pure α -lactalbumin protein(1mg/ml (b) AgNP complex.

LIST OF TABLES

Table 1. Zone of inhibition for antibacterial test of ZnO NP

Table 2. Zone of inhibition for antibacterial test of Ag NP

Table 3. Calculation of specific growth rate of *E.coli* in the presence of ZnO and Ag NP

Table 4. Size distribution and average size of protein, ZnO NP and conjugate.

Table 5. Size distribution and average size of protein, Ag NP and conjugate.

Table 6. Estimation of secondary structure components of pure α -lactalbumin protein and α -lac –AgNP complex by Circular Dichroism.

NOMENCLATURE

NP	Nanoparticle
ZnO	Zinc Oxide
Ag	Silver
XRD	X- ray diffraction
SEM	Scanning Electron Microscope
EDX	Energy dispersive X-ray spectroscopy
TGA	Thermal gravimetric analysis
DLS	Dynamic light scattering
CFU	Colony forming unit
PNPG	p-nitro phenyl- β -glucoside
PNP	p-nitro phenol
CD	Circular dichroism

CHAPTER-1

INTRODUCTION

1.1 Background

The field of nanotechnology is one of the most active research areas in modern materials science. Nanoparticles exhibit new or improved properties based on specific characteristics such as size, distribution and morphology. There have been impressive developments in the field of nanotechnology in the recent past years, with numerous methodologies developed to synthesize nanoparticles of particular shape and size depending on specific requirements. New applications of nanoparticles and nanomaterials are increasing rapidly.

Nanotechnology can be termed as the synthesis, characterization, exploration and application of nanosized (1-100nm) materials for the development of science. It deals with the materials whose structures exhibit significantly novel and improved physical, chemical, and biological properties, phenomena, and functionality due to their nano scaled size. Because of their size, nanoparticles have a larger surface area than macro-sized materials. The intrinsic properties of metal nanoparticles are mainly determined by size, shape, composition, crystallinity and morphology. Nanoparticles, because of their small size, have distinct properties compared to the bulk form of the same material, thus offering many new developments in the fields of biosensors, biomedicine, and bio nanotechnology. Nanotechnology is also being utilized in medicine for diagnosis, therapeutic drug delivery and the development of treatments for many diseases and disorders. Nanotechnology is an enormously powerful technology, which holds a huge promise for the design and development of many types of novel products with its potential medical applications on early disease detection, treatment, and prevention.

1.2 Zinc oxide nanoparticles

It usually appears as a white powder and is nearly insoluble in water. The powder is widely used as an additive for numerous materials and products including plastics, ceramics, glass, cement, rubber (e.g. car tyres), lubricants, paints, ointments, adhesives, sealants, pigments, foods (source of Zn nutrient), batteries, ferrites, fire retardants, etc. ZnO is present in the Earth crust as a mineral zincite; however, most ZnO used commercially is produced synthetically. ZnO is non-toxic and is compatible with human skin making it a suitable additive for textiles and surfaces that come in contact with human body. The increase in surface area of nanoscale ZnO compared to bulk has the potential to improve the efficiency of the material function.

1.2.1 Importance of ZnO nanoparticles

- 1) It is used in paints, cosmetics, sunscreens, plastic and rubber manufacturing, electronics and pharmaceuticals products etc.
- 2) It is also potentially used to treat leukemia and carcinoma cancer cell
- 3) It is also a strong antibacterial agent
- 4) It is also used as drug carrier
- 5) ZnO nanoparticles is also used in industrial sectors including environmental, synthetic textiles, food, packaging, medical care, healthcare, as well as construction and decoration.

1.2.2 Antibacterial activity of ZnO nanoparticles

Antibacterial agents are broadly of two types, organic and inorganic. At high temperatures/pressures organic antibacterial materials are found to be less stable compared to inorganic antibacterial agents. Thus Zinc Oxide has proved to be a powerful antibacterial agent

in the formulation of the microscale and nanoscale systems for therapeutic applications. ZnO nanoparticles showed greater antibacterial activity apparently than micro particles. The exact mechanisms of the antibacterial action have not yet been clearly identified.

ZnO particles have bactericidal effects on both Gram-positive and Gram-negative bacteria. They even have antibacterial activity against spores which are resistant to high-temperature and high pressure. From the literature it is evident that the antibacterial activity of ZnO nanoparticles depends on the surface area and concentration, while the crystalline structure and particle shape have little effect. Further it is also mentioned in the literature that smaller the size of ZnO particles better is its antibacterial activity. Thus higher the concentration and larger the surface area of the nanoparticles, the better is its antibacterial activity. The mechanism of the antibacterial activity of ZnO particles is still not well understood. Some researchers have proposed in their study that the generation of hydrogen peroxide is the main factor of the antibacterial activity, while it also indicated that the binding of the particles on the bacteria surface due to the electrostatic forces could be another factor.

This study is an investigation on the antibacterial activity of ZnO particles against pathogenic bacterial species like *Escherichia coli*, *Pseudomonas aeruginosa*, *Bacillus subtilis*, and *Streptococcus pneumonia*. We have opted these four different types of pathogenic bacteria because the following reasons-

- ***E. coli***: Gram- negative bacteria, virulent strain causes food poisoning, urinary tract infection, neonatal meningitis.
- ***Pseudomonas aeruginosa***: Gram-negative rod shaped bacteria infects the pulmonary tract, urinary tract, burns, wounds and also causes other blood infections.

- *Bacillus subtilis*: Gram-positive coccoid bacterium causes pneumonia, meningitis, sepsis.
- *Streptococcus pneumonia*: Gram-positive rod shaped bacteria causes food poisoning.

1.3 Silver Nanoparticles

Silver nanoparticles are one of the promising products in the nanotechnology industry. The development of consistent processes for the synthesis of silver nanomaterials is an important aspect of current nanotechnology research. One of such promising process is green synthesis.

Silver nanoparticles can be synthesized by several physical, chemical and biological methods. However for the past few years, various rapid chemical methods have been replaced by green synthesis because of avoiding toxicity of the process and increased quality.

1.3.1 Importance of Silver nanoparticles

- 1) It is used for purification and quality management of air, biosensing, imaging, drug delivery system.
- 2) Biologically synthesized silver nanoparticles have many applications like coatings for solar energy absorption and intercalation material for electrical batteries, as optical receptors, as catalysts in chemical reactions, for biolabelling, and as antimicrobials.
- 3) Though silver nanoparticles are cytotoxic but they have tremendous applications in the field of high sensitivity bimolecular detection and diagnostics, antimicrobials and therapeutics, catalysis and micro-electronics.
- 4) It has some potential application like diagnostic biomedical optical imaging, biological implants (like heart valves) and medical application like wound dressings, contraceptive devices, surgical instruments and bone prostheses.

- 5) Many major consumer goods manufacturers already are producing household items that utilize the antibacterial properties of silver nanoparticles. These products include nano-silver lined refrigerators, air conditioners and washing machines.

1.3.2 Silver nanoparticles as an antimicrobial agent

Ag NP highly antimicrobial to several species of bacteria, including the common kitchen microbe, *E. coli*. According to the mechanism reported, silver nanoparticles interact with the outer membrane of bacteria, and arrest the respiration and some other metabolic pathway that leads to the death of the bacteria.

New technology advances in reducing silver compound chemically to nanoscale sized particles have enabled the integration of this valuable antimicrobial into a larger number of materials—including plastics, coatings, and foams as well as natural and synthetic fibers. Nano-sized silver have already provides a more durable antimicrobial protection, often for the life of the product.

Current research in inorganic nanomaterials having good antimicrobial properties has opened a new era in pharmaceutical and medical industries. Silver is the metal of choice as they hold the promise to kill microbes effectively. Silver nanoparticles have been recently known to be a promising antimicrobial agent that acts on a broad range of target sites both extracellularly as well as intracellularly. Silver nanoparticles shows very strong bactericidal activity against gram positive as well as gram negative bacteria including multiresistant strains (Shrivastava et al., 2007), and also it was found to be in few studies (Zeng et al., 2007; Roe et al., 2008). Hence there is a huge scientific progress in the study of biological application of ZnO and Ag and other metal NP.

1.4 β -glucosidase

It is a hydrolytic enzyme which produces the monosaccharide/glucose in bacterial/yeast cells which helps in the metabolism process. Its activity assay protocol is very simple and it is industrially important enzyme also. In *E.coli* this enzyme is produced by activation of the lac operon. This enzyme plays an important role in the study of genetics and molecular biology. Since it is highly expressed and accumulates in lysozyme in aging cells, it is also used as an aging biomarker both *in vivo* and *in vitro* in qualitative and quantitative assays.

1.5 Study on the interaction of protein and Nanoparticles

The effect of the surface chemistry of biomaterials on the protein adsorption process has been a topic of great interest for many years. Protein adsorption to various materials has been widely studied and it has been found that factors such as electrostatic interactions, hydrophobic interactions, and specific chemical interactions between the protein and the adsorbent play important roles. These interactions with the surface can easily disrupt the native conformation and therefore, the protein function. On the other hand, the conjugation of protein with nanoparticles not only allows stabilization of the system, but more importantly, it also introduces biocompatible functionalities onto these nanoparticles for further biological interactions or coupling.

In our present investigation α -lactalbumin has taken as a key enzyme. Although the nanoparticles and protein interaction study was performed with few proteins like lysozyme, bovine serum albumin, β -lactalbumin, no interaction study was done with bovine α -lactalbumin. The protein is small and monomeric with a molecular mass of 14 kDa. The *in vitro* unfolding and refolding study of α -lactalbumin was done widely. However, it is worthy to know whether small nano

level metal particles can bring any changes its structure as well as function. Another importance of this protein is that in its intermediate state α -lactalbumin can be used as anti-turmeric agents. The same protein when form conjugate with fatty acid like oleic acid have been shown to act as anti-tumor agent.

Nanoparticles rapidly interact with the proteins present in various biological systems. However, to date, few studies have been conducted focusing on the nanoparticles that are commonly exposed to the general public, such as the metal/metal oxides. Therefore, understanding how and why proteins are adsorbed to these particles are important for understanding their biological response.

In our present investigation, we conducted an in-depth study on the synthesis and characterization of ZnO and Ag nanoparticles and their application on biological system. Antibacterial efficacy of the ZnO and Ag nanoparticles against four different bacteria like *Escherichia coli*, *Bacillus subtilis*, *Pseudomonas aeruginosa*, *Streptococcus pneumonia* has been performed. *In vivo* biological activity of expressed β -glucosidase enzyme in *E.coli* was measured in the presence of various concentrations of ZnO and silver nanoparticles. The interaction between α -lactalbumin protein and both ZnO and Ag nanoparticles were monitored in DLS particle size analyzer to confirm the formation of protein-NP conjugate. The structural change of the protein upon interaction with NP was monitored using tryptophan fluorescence and Circular dichroism spectroscopy.

CHAPTER-2

REVIEW OF LITERURE

2.1 History of Nanomaterials

Since many years, people have been preparing the glass windows with tiny colored metal particles especially silver which provide glassy yellow color (Solomon *et al.*, 2007).

2.2 Concept of Nanotechnology

The history of nanomaterials is quite long; nevertheless, major developments within nanoscience have taken place during the last two decades. The idea of Nanotechnology was first highlighted by Noble laureate Richard Feynman, in his famous lecture at the California Institute of Technology, 29th December, 1959. Richard Feynman in one of his articles published in 1960 titled, “There is plenty of room at the bottom” discussed the idea of nanomaterials. He pointed out that if a bit of information required only 100 atoms, then all the books ever written could be stored in a cube with sides 0.02 inch long. In 1970 Norio Taniguchi first defined the term Nanotechnology. According to him, “Nanotechnology mainly consists of the processing of, separation, deformation, and consolidation of material by one atom or by one molecule”. And in 1980 another technologist; K. Eric Drexler promoted technological significance in nano scale. The main important thing in nano dimension is the properties of particles are far different than bulk scale properties.

Nanoparticles are being used in different fields including electrical, biological textile and chemistry in which shape and size of colloidal metal particles play crucial role in different application including preparation of magnetic , electronic devices wound healing , anti microbial gene expression and in the preparation of bio composites. Noble metal colloids have the optical, catalytical electromagnetic properties which are dependent on size and shape of the

particles. The synthesis processes for the preparation of colloidal nanoparticles with controlled morphology is crucial.

2.3 Application of Nanoparticles

Once materials are prepared in the form of very small particles, they change significantly their physical and chemical properties. In fact in nano-dimension, percentage of surface molecule compare to bulk molecule is high and this enhances the activity of the particle in nano dimension and therefore, the normal properties of the particle like heat treatment, mass transfer, catalytic activity, etc are all increases. But compare to non-metal nanoparticles, metal nanoparticles have more industrial application. Nanoparticles offer many new developments in the field of biosensors, biomedicine and bio nanotechnology-specifically in the areas-

- Drug delivery
- As medical diagnostic tools,
- As a cancer treatment agent (Gold nanoparticles).

Nanoparticles and nanostructure are becoming a part in human medical application, including imaging or the delivery of therapeutic drugs to cell, tissues and organs. Drug loaded nanoparticles interact organ and tissues and are taken up by cells. Several studies have shown that the tissue, cell and even cell organelle distribution (Alexiou et al., 2000; Savic et al., 2003) of drugs may be controlled and improved by their entrapment in colloidal nanomaterials, mainly of the micellar structure, such as nanocontainer.

Magnetic nanoparticles have been receiving considerable attention because of their wide range of applications, such as the immobilization of the proteins and enzymes, bioseparation, immunoassays, drug delivery, and biosensors (Chen et al., 2002). Nanoparticles of ferromagnetic materials are of importance because of their reduced sizes that can support only single magnetic domains. The recent synthesis of arrays of 4 nm diameter FePt nanoparticles with an extremely narrow size distribution has promoted a significant research effort in this area, due to their potential technological application as recording media (Varlan et al., 1996).

2.4 Zinc oxide nanoparticles

The structure of zinc oxide surface has been computationally investigated using new atomistic potentials. The bulk termination is also subject to high concentrations of dimer vacancies which corresponds to fractional occupations in the surface layers. (Alexey A.Sokol and C.Richard et al., 2001). Mechanical properties such as internal stress or adhesion are important in order to guarantee the patterning accuracy and durability for various types of commercial applications.

2.4.1 Synthesis of ZnO nanoparticles

Oxide nanoparticles like ZnO NP can be synthesized by various techniques such as chemical vapor method, spray pyrolysis, laser synthesis techniques and vapor condensation method. Among these techniques available, the vapor condensation method have been considered to be the most attractive due to its robust and reliable control of the shape and size of the nanoparticles without requiring the expensive and complex equipments.

2.4.2 Application of ZnO

Zinc oxide (ZnO) is no stranger to scientific study. In the past 100 years, it has produced as a subject of thousands of research papers, dating back as early as 1935. For its potential of ultra violet absorbance, wide chemistry, piezoelectricity and luminescence at high temperatures, ZnO has entered into industry, and now is one of the critical building blocks in todays modern society. It is found in paints, cosmetics, plastic and rubber manufacturing, electronics and pharmaceuticals. More recently however, it has again gained large interest for its semiconducting properties (Look et al., 2001).

Among this oxide nanoparticles, ZnO nanostructure material has gained much interest owing to its wide applications for various devices such as solar cells, varistors, transducers, transparent conducting electrodes, sensors, and catalysts. However, these properties of the pure bulk ZnO are not stable and cannot meet the increasing needs for the present applications. In order to modify the properties of the ZnO, this semiconductor material was usually doped with some dopants such as Al, Si, and Ga. For example, Al-doped ZnO increases its conductivity without

impairing the optical transmission, which is regarded as a potential alternative candidate for ITO materials. (Zeng et al,2003)

Gas sensors based on ZnO had already been developed for detection and control of gases such as CO, H₂, H₂S, NH₃, etc. (Zhu et al,2005).

ZnO nanoparticles embedded in polymer matrices like soluble starch are a good example of functional nanostructures with potential for applications such as UV-protection ability in textiles and sunscreens, and antibacterial finishes in medical textiles and inner wears. ZnO nanoparticles has successfully been dispersed inside a soluble starch matrix using a simple water-based technique (Joshi M.et al., 2004). The stabilization of these nanoparticles was achieved by the presence of soluble starch in the reaction medium. The average size of the ZnO nanoparticles was estimated to be 38 ± 3 nm using a TEM (Vigneshwaran, 2006).

2.4.3 Antimicrobial potential of ZnO nanoparticles

It has already been shown that the nano-ZnO impregnated onto cotton textiles showed excellent antibacterial activity against two representative bacteria, *Staphylococcus aureus* and *Klebsiella pneumoniae* and promising protection against UV radiation. This work provides a novel and simple method for aqueous preparation of ZnO–soluble starch nanocomposites and their application onto cotton fabrics to impart antibacterial and UV protection functions (Vigneshwaran, 2006).

Zinc oxide (ZnO) is currently being investigated as an antibacterial agent in both microscale and nanoscale formulations (Nair and Sasidharan, 2009) Results have indicated that ZnO nanoparticles show antibacterial activity apparently greater than micro particles. While the exact

mechanisms of the antibacterial action have not yet been clearly understood, it has been suggested that the role of reactive oxygen species (ROS) generated on the surface of the particles, zinc ion release, membrane dysfunction, and nanoparticles internalization are the main cause of cell swelling (Nair et al., 2008).

High temperature treatment of ZnO particles has a significant effect on their antibacterial activity. Treatment at a higher temperature leads to a lower activity (Sawai et al., 1996a). The mechanisms of the antibacterial activity of ZnO particles are not well understood although (Sawai et al., 1996b, 1997, 1998) proposed that the generation of hydrogen peroxide be a main factor of the antibacterial activity, while (Stoimenov et al., 2002) indicated that the binding of the particles on the bacteria surface due to the electrostatic forces could be a mechanism (Sawai et al., 1996b) studied the antibacterial behaviour of ZnO particles by using a chemiluminescence and oxygen electrode analysis. They reported that H_2O_2 was produced in ZnO slurry and the concentration of H_2O_2 produced was linearly proportional to the ZnO particle concentration of the slurry. On the other hand, suggested that the electrostatic interaction between the bacteria surface and nanoparticles was a reason. The results obtained in this work clearly show that the presence of ZnO nanoparticles leads to damages the membrane wall of *E. Coli*. Such damages may be partly due to direct interactions between ZnO nanoparticles and bacteria membrane surface. ZnO nanoparticles used in this work are in the form of agglomerates with an average size greater than 200 nm. These large agglomerates are less likely to entered into the cell wall to damage the bacteria from the interior.

Metal nanoparticles are highly ionic and can be prepared with extremely high surface areas and with unusual crystal and morphologies that possess numerous edge/corner and other reactive surface sites. (Peter et al., 2002).

ZnO nanoparticles are being studied in combination with nonsurgical ablation regimens. In addition to better thermal effect on tumor ablation, nanoparticles can deliver anticancer therapeutics that show a synergistic antitumor effect in the presence of heat and can also be imaged to achieve precision in therapy. The molecular mechanism of nanoparticles mediated tumor ablation could further help engineer nanoparticles of appropriate composition and properties to synergize the ablation effect. The various types of nonsurgical tumor ablation method currently used in cancer treatment and potential improvements by nanotechnology application. (Manthe et al., 2010).

In the field of the research and development there are large amount of results obtained related to the ZnO nanoparticles, synthesis and its application. Preparation and utilization of ZnO nanoparticles are explored for the anti microbial effect in the fourth era. Due to the high polarity of the water, ZnO nanoparticles causes an immediate agglomeration during synthesis with water, which is a solvent system. Remedy was found for that, soluble starch was added before the reaction starts. The quick helical form of the soluble starch to protect and prevent the ZnO nanoparticles for agglomeration by action of steric hindrance (Vigneshwaran, 2006).

2.5 Silver Nanoparticles

The extraordinary optical properties of silver nanoparticles were used by glass founders as far back as in the time of the Roman Empire. This is evidenced by the so-called Lycurgus cup (4th century AD) now exposed in the British Museum. A detailed study of the composition of its

bronze-mounted insets of stained glass, carried out in the late 20th century, revealed the presence of metal nanoparticles (with the average diameter of 40 nm) that consists of silver (70 %) and gold (30 %) alloy (Barber, 1990). This explained a remarkable feature of this bowl to change its colour from red in transmitted light to grayish green in reflected light. In the preparation of this glass, nanosilver was formed insitu.

Before the 1980s, the scientific and practical interest in silver nanoparticles was exclusively caused by the possibility of their use as highly dispersed supports for enhancing the signals from organic molecules in the Raman spectroscopy (Creighton, et al., 1979; Lee et al., 1982). Fundamental studies carried out in the last three decade shows that silver nanoparticles exhibit a rare combination of valuable properties, namely, unique optical properties associated with the surface Plasmon resonance (SPR), well-developed surfaces, catalytic activity, high electrical double layer capacitance, etc.(Henglein, 1989). That's why they serve as a material in the development of new-generation electronic, optical and sensor devices. In the past 20 years, the trend miniaturization and the necessity of modernization of technological processes led to the substantial increase in the number of scientific publication devoted to the synthesis and properties of silver nanoparticles; at present, their synthesis is among the most actively developing trends of colloid chemistry.

Silver is widely used as a catalyst for the oxidation of methanol to formaldehyde and ethylene to ethylene oxide (Nagy et al., 1999). Colloidal silver is of particular interest because of distinctive properties, such as good conductivity, chemical stability, catalytic and antibacterial activity (Frattoni et al., 2005). For example, silver colloids are useful substrates for surface enhanced spectroscopy (SERS), since it partly requires an electrically conducting surface (Tessier et al., 2000; Rosi, et al., 2005).

2.5.1 Synthesis of Silver Nanoparticles

Material Scientists are conducting research to develop novel materials with better properties, more functionality and lower cost than the existing ones. Several physical, chemical and biological synthesis methods have been developed to enhance the performance of nanoparticles displaying improved properties with the aim to have a better control over the particle size, distribution and morphology (Granqvist et al., 1976; Shibata et al., 1998; Shankar, et al., 2003). Synthesis of nanoparticles to have a better control over particles size, distribution, morphology, purity, quantity and quality, by employing environment friendly economical processes has always been a challenge for the researchers (Hahn, 1997).

Chemical reduction is the most frequently applied method for the preparation of silver nanoparticles as stable, colloidal dispersions in water or organic solvents (Tao et al., 2006; Willy et al., 2006). Commonly used reductants are borohydride, citrate, ascorbate, and elemental hydrogen (Lee et al., 2003; Ahmadi, et al., 2003). The reduction of silver ions (Ag^+) in aqueous solution generally yields colloidal silver with particle diameters of several nanometers. When the colloidal particles are much smaller than the wavelength of visible light, the solutions have a yellowbrown color with an intense band in the 380–400 nm range and other less intense or smaller bands at longer wavelength in the absorption spectrum (Tessier et al., 2000; Cao et al., 2002; Rosi et al., 2005). This band is attributed to collective excitation of the electron gas in the particles, with a periodic change in electron density at the surface (surface plasmon absorption) (Henglein, 1989; Ershov et al., 1993).

Previous studies showed that use of a strong reductant such as borohydride, resulted in small particles that were somewhat monodisperse, but the generation of larger particles was

difficult to control (Creighton et al., 1994; Schneider et al., 1979). Use of a weaker reductant such as citrate, resulted in a slower reduction rate, but the size distribution was far from narrow (Shirtcliffe et al., 1999; Emory et al., 1997). Controlled synthesis of Ag NPs is based on a two-step reduction process (Schneider et al., 1979). In this technique a strong reducing agent is used to produce small Ag particles, which are enlarged in a secondary step by further reduction with a weaker reducing agent (Lee et al., 1982). Different studies reported the enlargement of particles in the secondary step from about 20–45 nm to 120–170 nm (Schneider et al., 1994; Schirtcliffe et al., 1999; Rivas et al., 2001). Moreover, the initial sol was not reproducible and specialized equipment was needed (Nickel et al., 2000). The synthesis of nanoparticles by chemical reduction methods are therefore often performed in the presence of stabilizers in order to prevent unwanted agglomeration of the colloidal silver Nanoparticle solution.

2.5.2 Biochemical Synthesis of Ag Nanoparticles

Chemical approaches are the most popular methods for the preparation of nanoparticles. However, some chemical methods cannot avoid the use of toxic chemicals in the synthesis protocol. Since noble metal nanoparticles such as gold, silver and platinum nanoparticles are widely applied to human contacting areas, there is a growing need to develop environmentally friendly processes of nanoparticles synthesis that do not use toxic chemicals. Biological methods of nanoparticles synthesis using microorganism (Nair et al., 2002), enzyme (Willner et al., 2006), and plant or plant extract (Shankar et al., 2004) have been suggested as possible ecofriendly alternatives to chemical and physical methods. Using plant for nanoparticles synthesis can be advantageous over other biological processes by eliminating the elaborate process of maintaining cell cultures (Shankar et al., 2004). It can also be suitably scaled up for large-scale synthesis of nanoparticles. It is well known that biological systems can provide a number of metal or metal-

containing particles in the nanometer size range. The synthesis of magnetite nanoparticles by magnetotactic bacteria (Lovely et al., 1987), siliceous materials by diatoms (Mann, 1993) and gypsum and calcium carbonate layers by S-layer bacteria (Pum et al., 1999) are some of the examples. The synthesis and assembly of nanoparticles would benefit from the development of clean, nontoxic and environmentally acceptable “green chemistry” procedures and involving organisms ranging from bacteria to fungi and even plants (Bhattacharya et al., 2005; Sastry et al., 2004). Hence, both unicellular and multicellular organisms are known to produce inorganic materials either intra-or extracellularly (Mann, 1996).

The *Verticillium* sp. fungal biomass when exposed to aqueous AgNO_3 solution resulted in the intracellular formation of silver nanoparticles, while *Fusarium oxysporum* biomass resulted in the extracellular silver nanoparticles (Senapati et al., 2004). The use of microorganisms such as bacteria, yeast, fungi and actinomycetes has been described for the formation of nanoparticles and their applications (Sastry et al., 2003; Mandal et al., 2006; Gericke and Pinches, 2006).

2.6 Application of Silver Nanoparticles

Silver nanoparticles have more applications in many areas, including biomedical, materials science, and catalysis. This is because of their unique properties when compared with their bulk solid. This part of the literature will give a brief description.

2.6.1 Human Health

Nanoparticles have many different effects on human health relative to bulk material from which they are produced (Albrecht, 2006). Increase the biological activity of nanoparticles can be beneficial, detrimental or both. Many nanoparticles are small enough to have an access to skin, lungs, and brain (Koziara et al., 2003; Oberdorster et al., 2004). Exposure of metal-containing nanoparticles to human lung epithelial cells generated reactive oxygen species, which lead to oxidative stress and damage of the cells (Limbach et al., 2007; Xi et al., 2006). A study on toxic effects of silver nanoparticles was done on zebrafish as a model due to its fast development and transparent body structure. The results show a deposition of particles on organs and severe developmental effects. The biocompatibility and toxicity of silver nanoparticles were exhibited by observing single silver nanoparticle inside embryos at each development stage. The types of abnormalities in zebra fish were strongly dependent on the dose of silver nanoparticles (Asharani, 2008).

2.6.2 Environmental

Silver nanoparticles are of great concern to wastewater treatment utilities and to biological systems. The inhibitory effects of silver nanoparticles on microbial growth were evaluated at a treatment facility using an extant respirometry technique. The nitrifying bacteria were susceptible to inhibition by silver nanoparticles, which could have detrimental effects on the microorganisms in wastewater treatment. The environmental risk of silver nanoparticles was recently investigated by determining released silver from commercial clothing. The sock material and wash water contained silver nanoparticles of 10–500 nm diameter.

2.6.3 Catalytic Action

High surface area and high surface energy predetermine metal nanoparticles for being effective catalytic medium. Growing small particles of silver have been observed to be more effective catalysts than stable colloidal particles. These growing particles catalyzed the borohydride reduction of several organic dyes. The reduction rate catalyzed by growing particles is distinctly faster compared to that of stable and larger silver particles, which are the final products of growing particles. Catalysis is due to efficient particle-mediated electron transfer from the BH_4^- ion to the dye. The catalytic activity of the particles depends on their size, $E_{1/2}$ of the dye, and the dye-particle interaction (Jana et al., 1999). Catalytic activity of silver nanoparticles can be controlled by its size, as redox potential depends on the nanoparticle size (Jana et al., 1999).

2.6.4 Antimicrobial

Silver is a non-toxic, safe inorganic antibacterial agent being used for centuries and is capable of killing about 650 microorganisms that cause diseases (Jeong et al., 2005). Silver has been described as being ‘oligodynamic’, that is, its ions are capable of causing a bacterostatic (growth inhibition) or even a bactericidal (antibacterial) impact. Therefore, it has the ability to exert a bactericidal effect at minute concentration (Percival et al., 2005). It has a significant potential for a wide range of biological application such as antibacterial agents for antibiotic resistant bacteria, preventing infections, healing wounds and anti-inflammatory (Taylor et al., 2005). Silver ions (Ag^+) and its compounds are highly toxic to microorganism exhibiting strong biocidal effect on many species of bacteria but have a low toxicity towards animal cells. Therefore, silver ions, being antibacterial component, are employed in formulation of dental

resin composites, bone cement, ion exchange fibers and coatings for medical devices (Panacek et al., 2005; Alt et al., 2004).

Bactericidal behavior of nanoparticles is attributed to the presence of electronic effects that are brought about as a result of change in local electronic structure of the surface due to smaller sizes. These effects are considered to be contributing towards enhancement of reactivity of silver nanoparticles surface. Silver in ionic form strongly interacts with thiol groups of vital enzymes and inactivates them. It has been suggested that DNA loses its replication ability once the bacteria are treated with silver ions (Morones et al., 2005). Silver nanoparticles destabilize plasma membrane potential and depletion of levels of intracellular adenosine triphosphate (ATP) by targeting bacterial membrane resulting in bacterial cell death.

Conventional compounds of silver such as silver nitrate and silver sulfadiazine are used to prevent bacterial growth in drinking water, sterilization and burn care. It is economical to consolidate silver in polymers, composites, fabrics and catheters for antibacterial functionality.

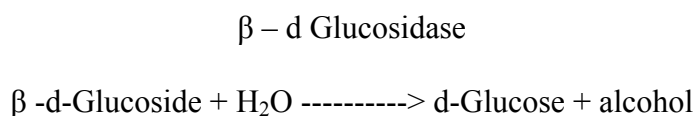
2.7 β -glucosidase

The term " β -glucosidase" defined here refers to β -glucoside glucohydrolase. Aroma of the wine can be attributed to the presence of many enzymes among which especially β -glucosidase of yeast plays crucial role in conversion of non volatile conjugates and sugar bounded conjugates into volatile compounds. Flavor is an important attribute of grape derived alcoholic beverages and many variables contribute to it. Among these, the enzymatic activity of β -glucosidase of yeast plays an important role as it is involved in either the expression of varietal and fermentative flavors or in their break down. . (Lomolino *et al.*, 2006).

β -Glucosidase (cellobiohydrolase) (EC 3.2.1.21), which catalyzes the hydrolysis of cellobiose into two molecules of glucose, is a main component of cellulase system (Xue et al., 1999). Most sources of study on the enzyme were from insect and bacterial sources (Gusakov et al., 2000 and Busto et al., 1996). The enzyme occurs in animals, plants, and microbes. A number of important physiological processes are mediated through these enzymes. The molecular weight of the enzyme has been found varies largely. Supplementing β -glucosidase in commercial cellulase preparations has been reported to result in increased rate of cellulose hydrolysis and ethanol production. Direct conversion of cellulose to ethanol has been demonstrated in recombinant *Saccharomyces cerevisiae* expressing heterologous genes of β -glucosidase (Haan et al., 2007).

S. cerevisiae is commonly used in wine production and able to influence aroma of the wine by hydrolysis of conjugated aroma precursors. The potential of aroma produced after the maturation of fruit is a crucial factor in wine production. From research it has been suggested that yeast strains can affect wine aroma as a result of the hydrolysis of conjugated aroma precursors. This aromatic potential is naturally revealed during fruit maturation by endogenous enzymes α - arabinosidase, α -rhamnosidase, β -glucosidases and possibly β -apiosidase. For complete hydrolysis of monoterpenes α 1-6 linkages must be cleared by different enzymes including α -arabinosidase, β -apiosidase, or α -L-rhamnosidase which produces monoterpenyl β -glucosidase finally produces monoterpenols by the action of β - glucosidase enzyme.

β -Glucosidase catalyzes the following reaction:



Even though *S. cerevisiae* produces β -glucosidase, it is observed that some amount of enzyme is lost into liquid media and therefore affecting the aromatic quality and flavor of the wine.

This enzyme has been studied extensively because of its important physiological function. However, the in vitro unfolding and refolding reports are not ample. Chen et al., in 2003 studied the unfolding process of BGL induced by guanidium hydrochloride and monitored by the measurement of biological activity and tryptophan fluorescence. However nanoparticle-mediated study of this enzyme is not known. Chien et al. reported that when Au and Ag nanoparticles were incorporated with yeast culture, a 3–5 fold enhancement in α -galactosidase was observed for intracellular activity as well as the secreted activity into the medium (Chien et al., 2007). But no such work was done in bacteria with a common recombinant gene like α -LA or large protein like BGL.

2.8 α -lactalbumin

α -lactalbumin is a small ($M_w=14.2\text{kDa}$), acidic (pH 4- 5), Ca^{2+} binding monomeric milk protein. It is the most abundant protein in human milk(Heine et al.,1991). α -LA performs an important function in mammary secretory cells as it is one of the components of lactose synthase complex which catalyzes the final step in lactose biosynthesis in the lactating mammary gland (Hill, 1975).

As α -lactalbumin possesses a strong Ca^{2+} binding site, it has been using as a model Ca^{2+} binding protein. It has several partially folded intermediate states, thus it is very attractive for folding and structural studies and used for the study of intermediate molten globule like states since, at acidic

pH and in the apo-state at elevated temperatures α -LA attains the classic 'molten globule' state. It has also been found from the reported literatures that some forms of α -LA can induce apoptosis in tumor cells which suggests that this protein has many important biological functions (Permyakov *et al.*, 2000).

2.8.1 Importance of α -lactalbumin

α -lactalbumin can be converted from the native state to a folding variant with modified biological function. The folding variant was found to induce apoptosis in tumor cells and immature cells, but healthy cells were not affected. Conversion to HAMLET (human α -lactalbumin made lethal to tumor cells) required partial unfolding of the protein and a specific fatty acid, C18:1, as a necessary cofactor. Astonishingly, native α -lactalbumin isolated from did not induce apoptosis. The difference in activity between the two forms of the protein was not caused by a change in secondary structure, but the active complex was found to have undergone a change in tertiary structure adopting a molten globule-like state (Svensson, 1999). The classical molten globule state of α -LA was studied extensively by many researchers (Dolgikh *et al.*, 1981) which is defined as a compact state with fluctuating tertiary structure. Molten globule state of α -LA retains a globular shape but is more swollen than the native state.

α -Lactalbumin, indeed, can be converted from the native conformation to the apoptosis inducing form and define the requirements for this structural and functional change. HAMLET (human α -

Lactalbumin made lethal to tumor cells) is shown to consist of partially unfolded α -Lactalbumin that has integrated a cofactor, which stabilizes the conformation.

2.9 Study of Protein-nanoparticle interaction

While binding of proteins to planar surfaces often induces significant changes in secondary structure, the high curvature of NPs can help proteins to retain their original structure. However, study of a variety of NP surfaces and proteins indicates that the perturbation of protein structure still happens to different extents. While various NPs have been used in the study of the interaction with proteins, ZnO and Au NPs have been used mostly. As a virtually inert and highly biocompatible nanomaterial, Au NPs exhibit enormous potential in biotechnology and biomedicine from protein and DNA detection to cancer therapy and drug delivery. While lysozyme is the protein has been studied most extensively, the similar kind of study has also been carried out with several other proteins, such as β -lactalbumin and bovine serum albumin, under similar conditions. The unfolding kinetics of lysozyme when adsorbed onto silica NPs or bovine serum albumin adsorbed on Au NPs surfaces, the proteins show a rapid conformational change at both secondary and tertiary structure levels (Vertegel et al., 2004; Wu and Narsimhan, 2008; Bhattacharya et al, 2007). Most of the studies have reported that loss of α -helical content occurs as detected by circular dichroism spectroscopy when proteins are adsorbed onto NPs and a significant increase in sheet and turn structures.

Chakraborti et al., 2009 showed that when lysozyme interacts with ZnO NPs, it retains high fraction of its native structure with negligible effect on its activity upon attachment to NPs. Compared to the free protein, lysozyme-ZnO conjugates are more stable in the presence of

chaotropic agents (guanidine hydrochloride and urea) and also at elevated temperatures. There is an approximately 4% increase of the helical content (at the expense of random coil structures) of lysozyme in the presence of NPs was also reported recently.

Shang et al., 2007 showed that the unfolding of Rnase A on spherical silica NPs was strongly affected by the size, and hence surface curvature, of the support. The enzyme was less stable on NP surfaces than in free solution, and the stability was decreased further on larger particles with smaller surface curvature. Although the protein may retain most of its native structure after adsorption on the NP surface, in some cases the thermodynamic stability of the protein is decreased, making the protein more sensitive to chemical denaturants such as urea (Shang et al., 2007a).

Recent study reported that some nanomaterials catalyze the formation of protein fibrils as evidenced from the fact that interactions between proteins and nanophase materials could induce modifications in protein structure, leading to the growth of extended assemblies (Zhang et al., 2009).

In addition, another recent study have characterized how the effect of protein concentration at the NP surface influences affect on protein structure and function (Shang et al., 2007b; Wu and Narsimhan, 2008).

2.10 Motivation of the present work

Among the different methods for NP synthesis, the chemical reduction method and green synthesis method were widely studied method due to its advantage in controlling particle size, morphology very effectively. This method also less time consuming process for getting the desired nanoparticles size. Although there have been ample informations about the antimicrobial effects of ZnO and Ag NP against many bacteria. These studies were not carried out with various sized NP against human pathogenic bacteria.

Moreover, despite the unbelievable speed of development of nano science, relatively few information is available about the effect of the surface chemistry of nanoparticles on the biomolecules conjugation process and their subsequent consequences. Many nanoparticles have been used as drug carriers in human, however, their interaction with thousand of proteins have not been predicted yet. It is essential to know the consequence of the protein in terms of their structure and function when they interact with nanoparticle *in vivo*. Moreover, nanoparticle-mediated cell death needs a detail understanding about the consequence of proteins conformation and biological function when NP enters through cell membrane and interact with them.

This is also essential to know the effect of nanoparticle in gene expression level *in vivo*. Because many enzymes are expressed at a lower level and there has been a great effort to enhance the activity/expression level of many enzyme industrially using molecular or chemical chaperones. However, nanoparticles have been not used to observe any such effect so far.

2.11 OBJECTIVES:

1. Synthesis and details characterization of ZnO (chemical reduction method) and silver nanoparticles (by green synthesis method).
2. Examine the antimicrobial activity/potential of ZnO and Ag nanoparticles against the four different human pathogenic bacteria like ; *E. coli*, *Pseudomonas aeruginosa*, *Bacillus subtilis*, *Streptococcus pneumonia*.
3. Investigate the *in vitro* physical interaction of ZnO and Ag nanoparticles with α -lactalbumin protein monitored by DLS particle size analyzer, fluorescence and circular dichroism spectroscopy.

CHAPTER-3

MATERIALS AND METHOD

3.1 General:

Preparation and utilization of ZnO and Ag nanoparticles have been explored widely observe to the anti microbial effect in the fourth era. Synthesis of ZnO without using a protective agent was a problem. Due to the high polarity of the water, ZnO nanoparticles cause an immediate agglomeration during synthesis with water due to the Vander wall forces of attraction. To prevent aggloromation, soluble starch is now added before the reaction. The quick helical forms of the soluble starch protect and prevent the ZnO nanoparticles from agglomeration by the action of steric or electrostatic hindrance and stabilizing the ZnO nanoparticles. ZnO was used in paints, cosmetics, sunscreens, plastic and rubber manufacturing, electronics and pharmaceuticals products etc. It is also a strong antibacterial agent (Reddy et al., 2007; Appl. Phys. Lett.).

In recent years silver nanoparticles have been investigated by many research groups nationally and internationally. It is mainly because of the potential application of nanomaterials in biology, medicine, optics and in modern electronic devices (Xue et. al., 2003). Silver nanoparticles have advantage over other noble nanoparticles (e.g., gold and copper) because the surface Plasmon resonance energy of silver is situated far from the interband transition energy. Silver nanoparticles exhibit very strong bactericidal activity against gram-positive as well as gram-negative bacteria including multiresistant strains, as well as potential antifungal agent. (Shrivastava, et al. 2007).

3.2 Chemicals:

Pure and analytical grade chemicals were used in all experiments including synthesis of ZnO and silver nanoparticles, media preparation for growth of bacterial cells. Zinc nitrate hexahydrate, sodium hydroxide (NaOH) starch and silver nitrate (AgNO_3), were purchased from Himedia laboratories Pvt. Ltd., Mumbai, India. The bacterial cultures of *E.coli*, *Bacillus subtilis*, *Pseudomonas aeruginosa*, *Streptococcus pneumonia* were obtained from National Center For Cell Science (NCCS), Pune. Antibiotics, (Ampicilin, Tetracycline, Ciprofloxacin, and Tobramycin) were purchased from Himedia, Mumbai, India. Beef extract, peptone, sodium chloride (NaCl) were purchased from Merck, India.

3.3 Glassware and Apparatus

All glass wares (Conical flasks, Measuring cylinders, Beakers, Petri plates and Test tubes etc.) were purchased from borosil, India.

3.4 Synthesis of ZnO nanoparticles

The ZnO nanoparticles were prepared by wet chemical method using zinc nitrate and sodium hydroxides precursors and soluble starch as stabilizing agent. Soluble starch (0.5%) was dissolved in 500 ml of distilled water and treated in microwave oven (Samsung, Model No-CE103VD) for complete solubilization. Zinc nitrate, 14.874 g (0.1 mol), was added in the above solution. Then the solution was kept under constant stirring at room temperature using magnetic stirrer (Tarson spinnot digital) for one hour. After complete dissolution of zinc nitrate, 300ml (0.2 mol), of sodium hydroxide solution was added under constant stirring, drop by drop touching the walls of the vessel. The reaction was allowed to proceed for 2 h after complete

addition of sodium hydroxide. After the completion of reaction, the solution was allowed to settle for overnight and the supernatant solution was then discarded carefully. The remaining solution was centrifuged (Remi cooling centrifuge instrument, Model No-C30BL) at $10,000 \times g$ for 10 min and the supernatant was discarded. Thus produced nanoparticles were washed three times using distilled water. Washing was carried out to remove the byproducts and the excessive starch that were bound with the nanoparticles. After washing, the nanoparticles were dried at 80°C for overnight. During drying, complete conversion of $\text{Zn}(\text{OH})_2$ into ZnO takes place.

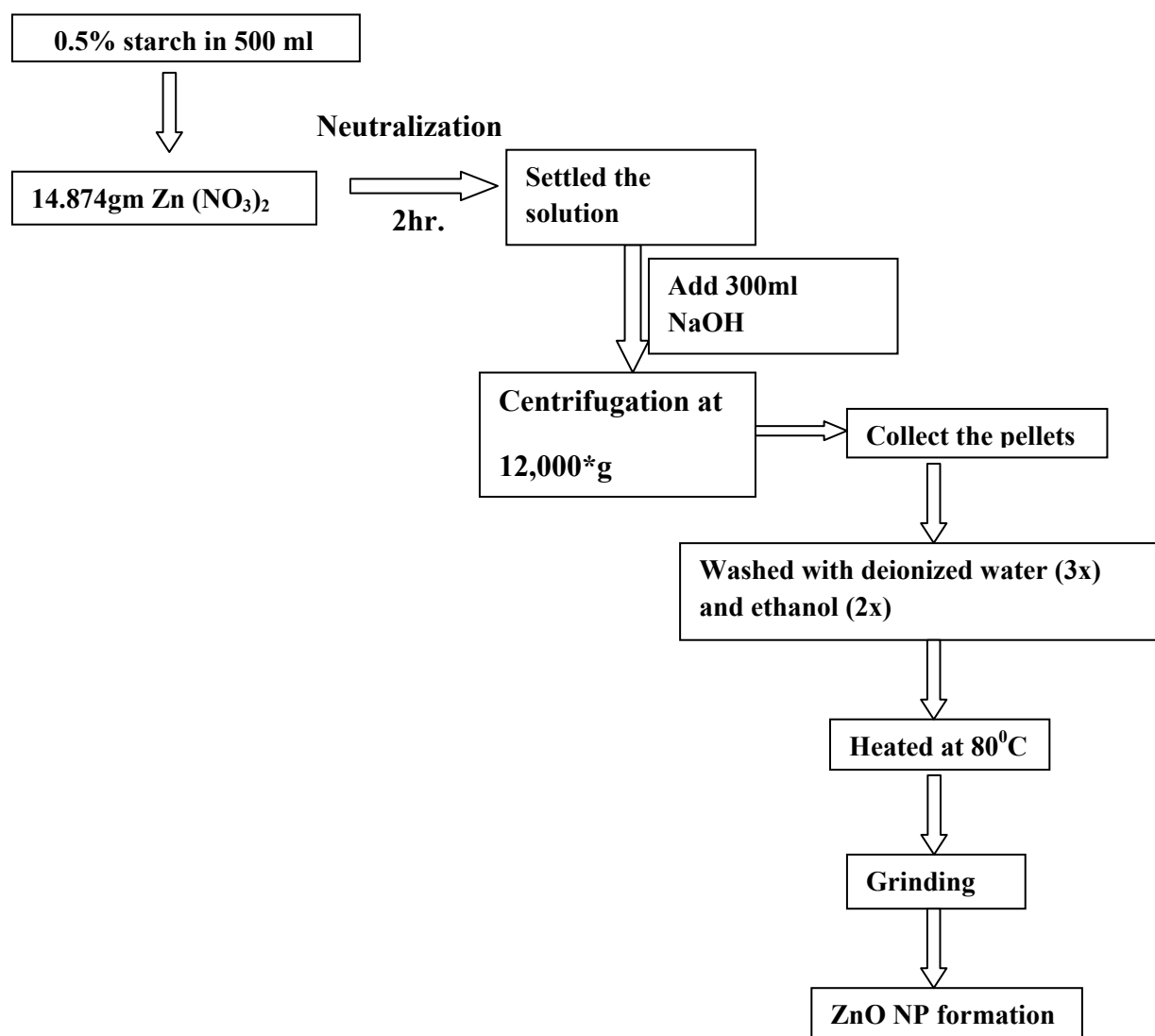


Figure 1. Schematic diagram of synthesis of ZnO sample

3.5 Synthesis of silver nanoparticles from *Citrus Sinensis* fruit extract

3.5.1 Preparation of the Extract

Weighing 25 g of *Citrus Sinensis* was thoroughly washed in distilled water, dried, cut into fine pieces and was smashed into 100 ml sterile distilled water and filtered through Whatman No.1 filter paper (pore size 0.45 μm) and was further filtered through 0.22 μm sized filters. The extract was stored at 4⁰ C for further experiments.

3.5.2 Synthesis of Silver nanoparticles from *Citrus Sinensis* extract

The aqueous solution of 1mM silver nitrate (AgNO_3) was prepared and used for the synthesis of silver nanoparticles. 10 ml of *Citrus Sinensis* extract was added into 90 ml of aqueous solution of 1 mM silver nitrate for reduction into Ag^+ ions and kept for incubation period of 15 h at room temperature. Here the filtrate act as reducing and stabilizing agent for 1 mM of AgNO_3 .

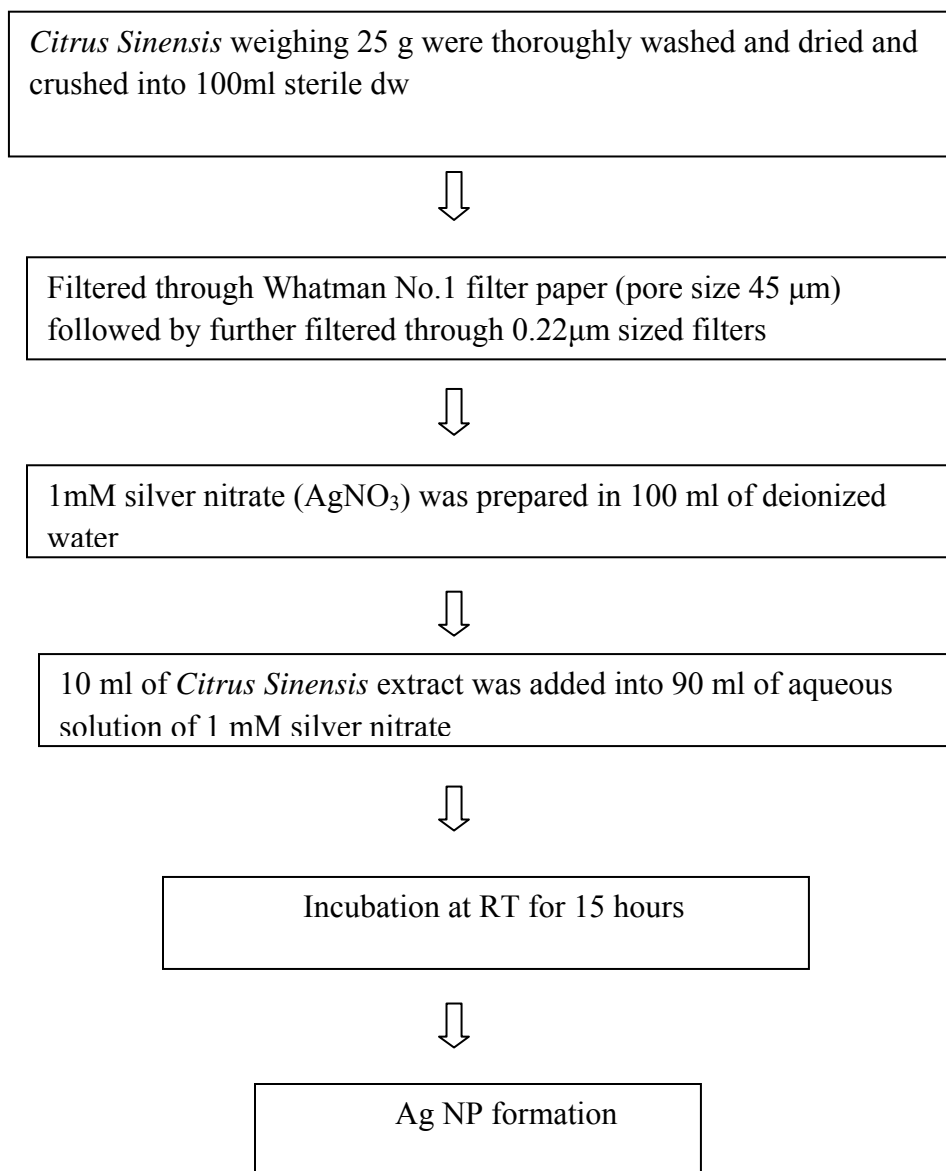


Figure 2. Schematic diagram of synthesis of Ag NP.

3.6 Characterization techniques:

3.6.1 UV-Vis Spectroscopy-

The ZnO and Ag nanoparticles were characterized in a Perkin-Elmer UV-VIS spectrophotometer, Lambda-19 to know the kinetic behavior of ZnO and Ag nanoparticles. The scanning range for the samples was 200-800 nm at a scan speed of 480 nm/min. The spectrophotometer was equipped with “UVWinlab” software to record and analyze data. Base line correction of the spectrophotometer was carried out by using a blank reference. The UV-Vis absorption spectra of all the samples were recorded and numerical data were plotted in the “Origin 6.5”.

3.6.2 X-RAY Diffraction method

The phase evolution of calcined powder as well as that of sintered samples was studied by X-ray diffraction technique (Philips PAN analytical, The Netherland) using Cu K α radiation. The generator voltage and current was set at 35 KV and 25 mA respectively. The ZnO and Ag samples were scanned in the 2θ ranges 15 to 70 $^{\circ}$ C range in continuous scan mode. The scan rate was 0.04 $^{\circ}$ /sec.

Phases present in the sample has been identified with the search match facility available with Philips X’pert high score software.

The crystallite size of the calcined powders was determined from X-ray line broadening using the Scherrer's equation as follows:

$$t = \frac{0.9\lambda}{B \cos \theta} \quad \text{----- (1)}$$

Where,

t = crystallite size,

λ = wavelength of the radiation,

θ = Bragg's angle and

B = full width at half maximum

3.6.3 Scanning electron microscope (SEM)

In this research work, Jeol JSM-6480 LV SEM machine were used to characterize mean particle size, morphology of nanoparticles. The ZnO powder sample and freeze dried sample of Ag NP solution was sonicated with distilled water, small drop of this sample was placed on glass slide allowed to dry. A thin layer of platinum was coated to make the samples conductive Jeol JSM-6480 LV SEM machine was operated at a vacuum of the order of 10^{-5} torr. The accelerating voltage of the microscope was kept in the range 10-20 kV. Compositional analysis on the sample was carried out by the energy dispersive X-ray spectroscopy (EDS) attached with the SEM. The EDX analysis of ZnO and Ag sample was done by the SEM (JEOL-JSM 5800) machine. The EDX normally reveals the presence of phases.

3.6.4 DLS particle size analyzer

A laser diffraction method with a multiple scattering technique has been used to determine the particle size distribution of the powder. It was based on Mie-scattering theory. In order to find out the particles size distribution the ZnO and Ag powder was dispersed in water by horn type ultrasonic processor [Vibronics, model:VPLP1].Then experiment was carried out in computer controlled particle size analyzer [ZETA Sizers Nanoseries (Malvern Instruments Nano ZS)] to find out the particles size distribution.

3.6.5 Thermo gravimetric analysis (TGA)

Thermal decomposition behavior of the gel has been studied using Netzsch (STA 449C) DSC/TG. The DSC/TG patterns were collected as a function of temperature up to 900oC under N₂ atmosphere. The heating rate was 10oC/min. in N₂. Alpha alumina was used as reference material.

3.7 Antibacterial test

3.7.1 Growth inhibition in liquid medium-

The antibacterial effect of both ZnO and silver nanoparticles, both in liquid nutrient growth medium and on agar plates were studied. *E. coli* culture in nutrient media (1g yeast extract, 1 g beef extract, 0.5 g NaCl, dissolved in 100 ml distilled water), were used for both

studies. Frozen *E. coli* cells were grown overnight in the nutrient medium to prepare inoculum. The bacteria cultures were allowed to grow in a shaking incubator at 310 K (37°C), and 200 rpm. ZnO and silver NP were dispersed in autoclaved deionized water by ultrasonication. Aqueous dispersion of silver nanoparticles of desired concentration was made. For this experiment, freshly grown bacterial inoculums (10^4 cells/ml) of *E.coli* was incubated in the presence of a range of ZnO nanoparticles with concentration of 0, 5mM, 10mM, and 15mM that added in each flask to observe the bacterial cell growth pattern at 310 K (37°C) and 150 rpm. Similarly silver nanoparticles of 0, 0.2mM, 0.3mM and 0.6mM concentration added in each flask to observe the bacterial cell growth pattern under the same condition. Total solution volume used in each flask was 50 ml. In liquid medium, growth of *E. coli* was indexed by measuring optical density (OD). Optical density measurements on the samples collected from the solution were carried out at λ_{max} = 600 nm against growth media control by UV-Vis spectroscopy after every 2 h time interval and up to 24 h. Control flask obtained 50 ml of all the initial reaction components except the nanoparticles. The specific growth rate of the bacterial culture was calculated using the following equation-

$$\mu = \ln (m_2/m_1)/t_2-t_1.$$

Where μ is specific growth rate, m_1 and m_2 is the biomass produced at time t_1 and t_2 of the bacterial culture.

3.7.2 Disc Diffusion Method

The antibacterial assays were also performed by standard disc diffusion method. Nutrient broth/agar (1g beef extract, 1g peptone, 0.5 g NaCl dissolved in 100 ml of double distilled water) was used to cultivate bacteria. The media was autoclaved and cooled. The media was poured in

the petri discs and kept for 30 minutes for solidification. After 30 minutes the fresh overnight cultures of inoculum (100 μ l) of four different culture were spread on to solidified nutrient agar plates. Sterile paper discs made of Whatman filter paper, 5 mm diameter (dipped in 50 mg/liter ZnO and silver nanoparticles) along with four standard antibiotic containing discs were placed in each plate. The cultured agar plate were incubated at 37⁰C (310K) for 24 h. After 24 h of incubation the zone of inhibition was investigated.

3.7.2 CFU Measurement

E.coli was used for colony forming units (CFU) measurements on the solid medium plate. Samples treated with different concentrations of ZnO (50,100,150 μ g/ml) and Ag nanoparticles (0, 20, 30, 60 μ g/ml) were spread on nutrient agar plates. These samples were diluted at 10⁹ folds to get the better colonies. After incubation at 37⁰C (310K) for 24 h, the numbers of CFU were counted.

3.8 Effect of NP on *in vivo* gene expression level in *E.coli*:

3.8.1 Quantitative assay of β -glucosidase activity

250 ml of *E.coli* culture was grown at 25⁰ C for 72 h and centrifuged at 4500 rpm for 10 minutes at 4⁰C. The pellet was washed with chilled PBS of 10 ml and the sample was sonicated. Sonicated sample was centrifuged at 10000rpm and 4⁰C, the supernatant was separated. 100 μ l of that was added in each flask along with 100 μ l of citrate phosphate buffer (0.1M, pH5). This was followed by addition of 100 μ l of 0.55×10^{-2} M of pNPG and incubated at 37⁰ C for 30 minutes. After

incubation, 1M sodium carbonate was added to stop the reaction allowing the yellow color of the *p*-nitrophenolate ion to develop and 2.0 ml of ethanol was added. This was followed by centrifugation at 10000 rpm for 15 minutes. The supernatant was taken and the optical density of each sample of measured to know the relative β -glucosidase activity.

In the presence of enzyme β -glycosidase enzyme, the substrate *p*-nitrophenyl- β -glucoside (pNPG) is converted into the products *p*-nitrophenol (PNP) and glucose. This reaction can be monitored by the change in color from colorless to yellow colored solution.

3.9 Formation of α -lactalbumin and silver nanoparticles complex monitored by DLS particle size Analyzer:

α -lactalbumin solution was prepared by dissolving the protein in 100ml in PBS to a concentration of 5mg/ml and it is added 1000 μ l of the protein solution to pre-synthesized silver nanoparticles solution. Here 935 μ l of Ag nanoparticles was added with 65 μ l of protein to make up the volume to 1ml and this was incubated with 1mM silver nanoparticles for 10mins. After the incubation formation of α -lactalbumin and silver nanoparticles binary complex was monitored by DLS particle size Analyzer.

3.10 *In vitro* interaction study of silver nanoparticles and α -lactalbumin monitored by spectroscopic techniques

3.10.1 Fluorescence emission spectra of tryptophan residues in bovine α -lactalbumin

Bovine α -lactalbumin was dissolved in phosphate-buffered saline (PBS: 150 mM NaCl, 1.9 mM NaH_2PO_4 , 8.1 mM Na_2HPO_4 , pH 7.4) at a concentration of 0.2mg/ml.

Fluorescence spectra were taken with a Perkin-Elmer LS-55 Luminescence spectrometer. The experiment was performed at 25 °C. The excitation spectrum was measured in the wavelength range of 200-3000 nm with $\lambda_{\text{max}}^{\text{ex}}$ of 280nm. The emission spectra were recorded from 300 to 400 nm. The excitation and emission slit widths were set to 10 and 5.0 nm, respectively. Samples were contained in 1 cm path length quartz cuvettes. Base-line corrections were done with only buffer (without) protein in all cases. Before examining the fluorescent properties of the protein, it was checked that silver nanoparticles did not exhibit fluorescence at 300–440 nm.

3.10.2 Quenching studies of bovine α -lactalbumin

Fluorescence quenching experiments were carried out by the addition of a small aliquot of acrylamide stock solutions (4M) to the protein solution, previously incubated at pH 7.0 at 37°C for 1 h and the intrinsic tryptophan fluorescence intensities were recorded (λ_{ex} , 280 nm; λ_{em} , 346.5 nm). The intrinsic tryptophan fluorescence intensities were measured at $\lambda_{\text{max}}^{\text{em}} = 346.5$ nm emission wavelengths for 280 nm excitation wavelength (λ_{ex}) for all bovine α -lactalbumin samples and plotted.

3.10.3 Far-UV CD measurement

Circular Dichroism (CD) spectra of 1 mg/ml bovine α -lactalbumin was recorded using a JASCO J-810 CD polarimeter (JASCO, Tokyo, Japan). The buffer used for the measurement was 10 mM sodium cacodylate, pH 7.0. Each spectrum represented the average of three accumulations recorded between wavelengths of 200 and 250 nm, with a 0.2 nm resolution, a bandwidth of 0.5 nm, a response time of 4 s, sensitivity of 100 mdeg, and a scan speed of 20 nm/min using a cuvette of path length of 0.2 cm. All spectra were corrected for background by

the subtraction of the buffer blank. All measurements were made at 25°C. The CD signal obtained from the instrument had the unit in mdeg. The values in mdeg were converted to molar residue ellipticity by using the molecular weight and concentration of protein solution with the help of software associated with the instrument.

The molar residue ellipticity (θ) was calculated using the formula:

$$[\theta] = (\theta_{\text{obs}} \text{ in mdeg}) / (\text{Molar conc}^n \text{ of the protein} \times \text{path length in mm} \times \text{number of amino acid residue present in the protein})$$
 (Yang et al., 1986).

The CD intensities were expressed as molar residue ellipticity (MRE) with the unit $\text{deg.cm}^2.\text{dmol}^{-1}$. The percentages of the different secondary structure components (α -helix, β -sheet and random coil) were estimated (prediction errors on the range of 200–250 nm were 5%) in online k2D software (Andrade et al., 1993; Merelo et al., 1994).

CHAPTER-4

RESULTS AND DISCUSSION

4.1 Synthesis and Characterization of ZnO and Ag nanoparticles

4.1.1 Synthesis of ZnO by chemical reduction method

ZnO nanoparticle was synthesized according to the protocol discussed in the ‘Material and Methods’ (Section 3.4). The powder form nanoparticles looks white in colour as in Figure 3.



Figure 3. Synthesized ZnO powder by chemical reduction method

4.1.2 Synthesis of Ag nanoparticles by green synthesis process (from *Citrus sinensis*)

Ag nanoparticles exhibit yellowish brown color in aqueous solution due to excitation of surface Plasmon resonance. On mixing the extract with aqueous solution of the Ag ion complex, a change in

the color from colorless to yellowish brown was observed. It was due to the reduction of Ag^+ which indicates the formation of Ag nanoparticles shown in Figure 4.

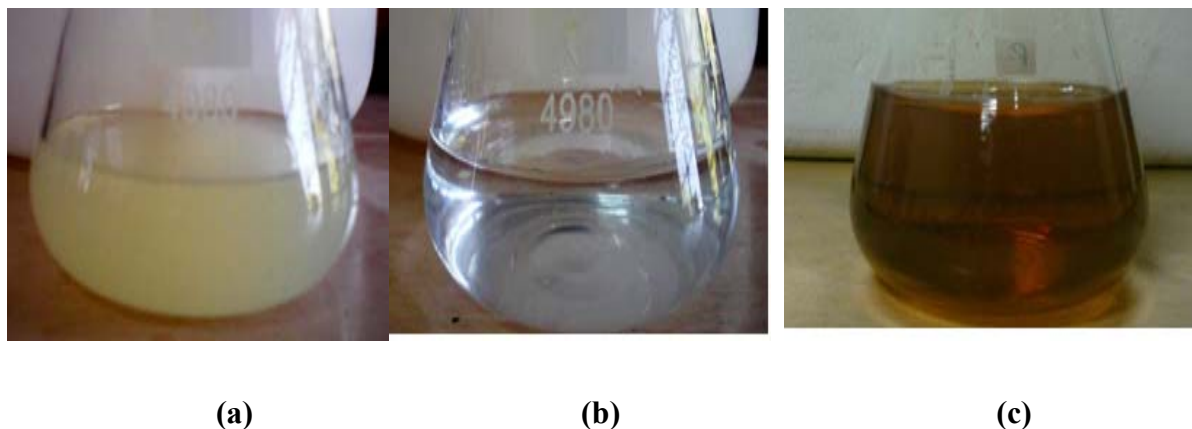


Figure 4. Digital photographs of (a) *Citrus sinensis* extract (b) 1 mM AgNO_3 without *Citrus sinensis* extract (c) 1 mM AgNO_3 with *Citrus sinensis* extract after 10 hrs of incubation.

4.2 Characterization of ZnO and Ag nanoparticles

4.2.1 UV–Vis spectral analysis

The UV-Vis spectra of ZnO NP prepared with 0.5% concentration of soluble starch was shown in Figure 5 (a). The absorption peak of the prepared nano ZnO was found at around 360 nm.

The UV-Vis absorption spectra of the Ag NP were shown in Figure 5 (b). Absorption spectra of Ag nanoparticles formed in the reaction media has absorbance maxima at 421 nm. A remarkable broadening of peak at around 350 nm to 480 nm indicates that the particles are polydispersed. It was observed that the peak was blue shifted in the absorption spectrum from 350nm to 480 nm with increasing reaction time.

The ZnO spectra obtained was followed the reported result published by (Vigneswaran et al., 2006).

Also the spectra of Ag nanoparticles followed the reported result published by Jain et al., 2009.

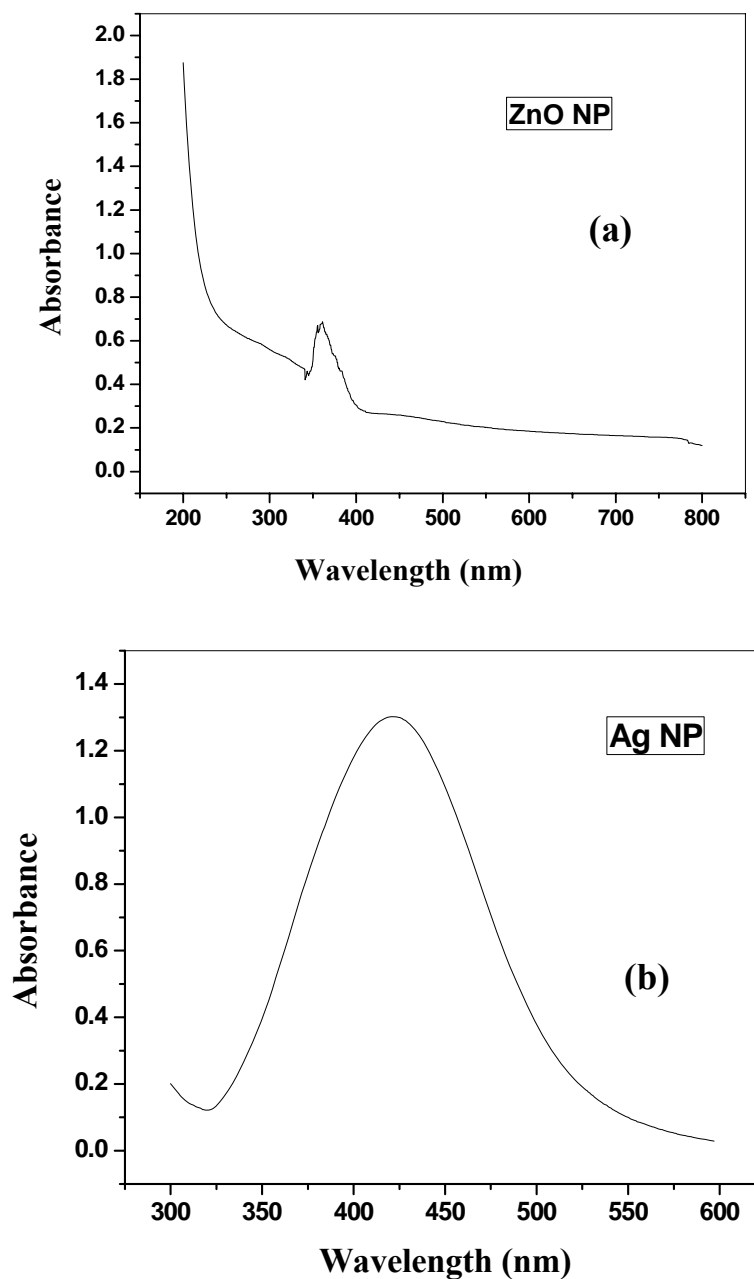


Figure 5. (a) UV-Vis spectra of the ZnO and (b) Ag nanoparticles prepared with 0.5% of soluble starch and 1mM aqueous AgNO₃ solution with 10% *Citrus sinensis* extract.

4.2.2 X-ray diffraction pattern for ZnO and Ag nanoparticles

The XRD pattern of bulk ZnO and nano ZnO were presented in Figure 6 (a). All the peaks were hexagonal and approximately close to the reported information (jcpds-79-0206). Due to the crystal symmetry and related face velocities, the common crystal habit of ZnO is hexagonal in shape. Also the ZnO NP is the thermodynamically stable crystallographic phase. The width of the peaks in case of ZnO NP has increased due to the quantum size effect. The average particle size was estimated to be 42 nm using Scherer equation (discussed in ‘Material and Methods’ section 3.6.2).

The *Citrus sinensis* extract-mediated synthesized Ag nanostructure was confirmed by the characteristic peaks observed in the XRD image which was shown in Figure 6 (b). All diffraction peaks correspond to the characteristic face centered cubic (FCC) silver lines. These diffraction lines observed at 2θ angle 32.8° , 38.2° , 55.10° and 65.7° respectively, have been indexed as (111), (200), (220) and (311) respectively. XRD patterns were analyzed to determine peak intensity, position and width, full-width at half-maximum (FWHM) data was used with the Scherer formula explained in section materials and method. The typical XRD pattern revealed that the sample contains a mixed phase (cubic and hexagonal) structures of silver nanoparticles. The average estimated particle size of this sample was 50 nm derived from the FWHM of peak corresponding to 111 plane with cubic and hexagonal shape.

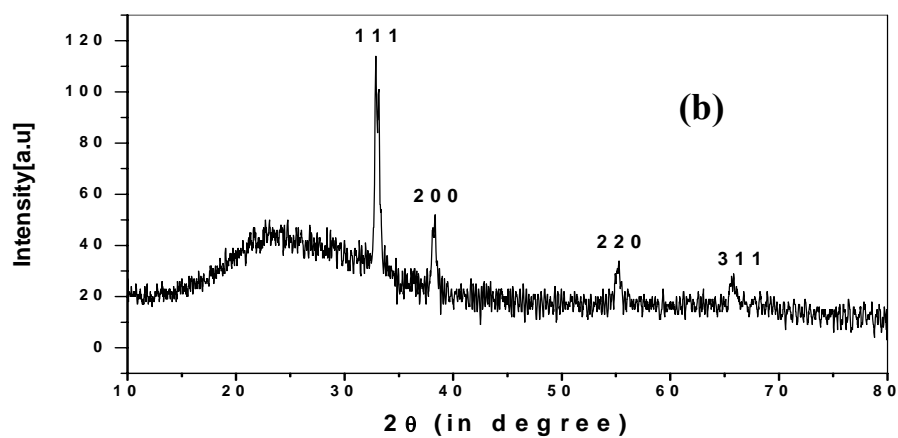
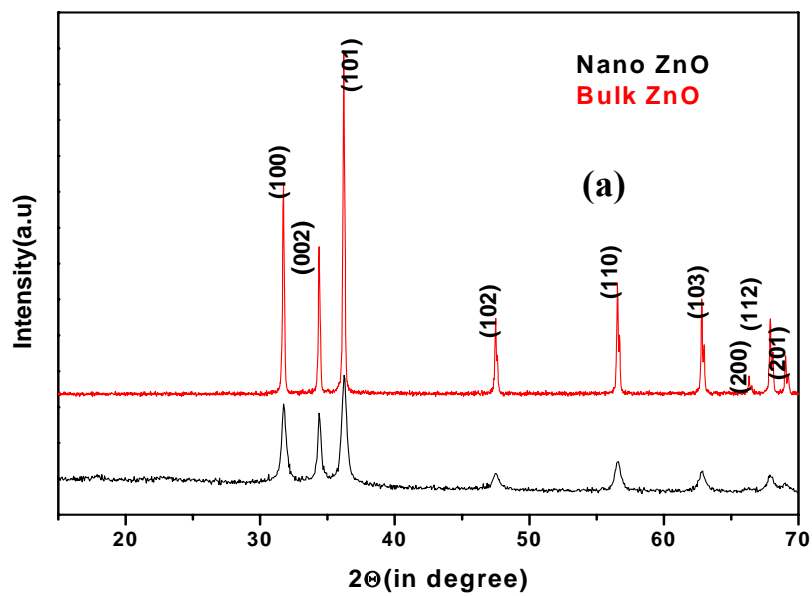


Figure 6. (a) XRD patterns of ZnO nanoparticles (red) bulk ZnO (black) ZnO synthesized using 0.5% starch. The peaks assigned to diffractions from various planes are of hcp ZnO. (b) The Ag nanoparticles synthesized by treating 10% *Citrus sinensis* extract with 1 mM aqueous AgNO₃ solution.

4.2.3 SEM Analysis of ZnO and Ag Nanoparticles

The SEM image of ZnO and Silver nanoparticles synthesized by chemical reduction method and green synthesis process by using 10 % fruit extract and 1mM AgNO₃ concentration was shown in Figure 7. It gave a clear image of highly dense ZnO and silver nanoparticles. The SEM image showing silver nanoparticles synthesized using *Citrus sinensis* extract confirmed the development of silver nanostructures.

4.2.4 EDX analysis of ZnO and Ag nanoparticles

Figure 7 shows the EDX plot of SEM image of ZnO and Ag nanoparticles. The EDX reading proved that the required phase of zinc (Zn) and oxygen (O) is present in the sample. The graph also shows the presence of carbon (C), silicon (Si) and calcium (Ca) are present in the EDX picture of silver nanoparticles. This is probably due to the presence of substrate over which the NP sample was held during SEM microscopy.

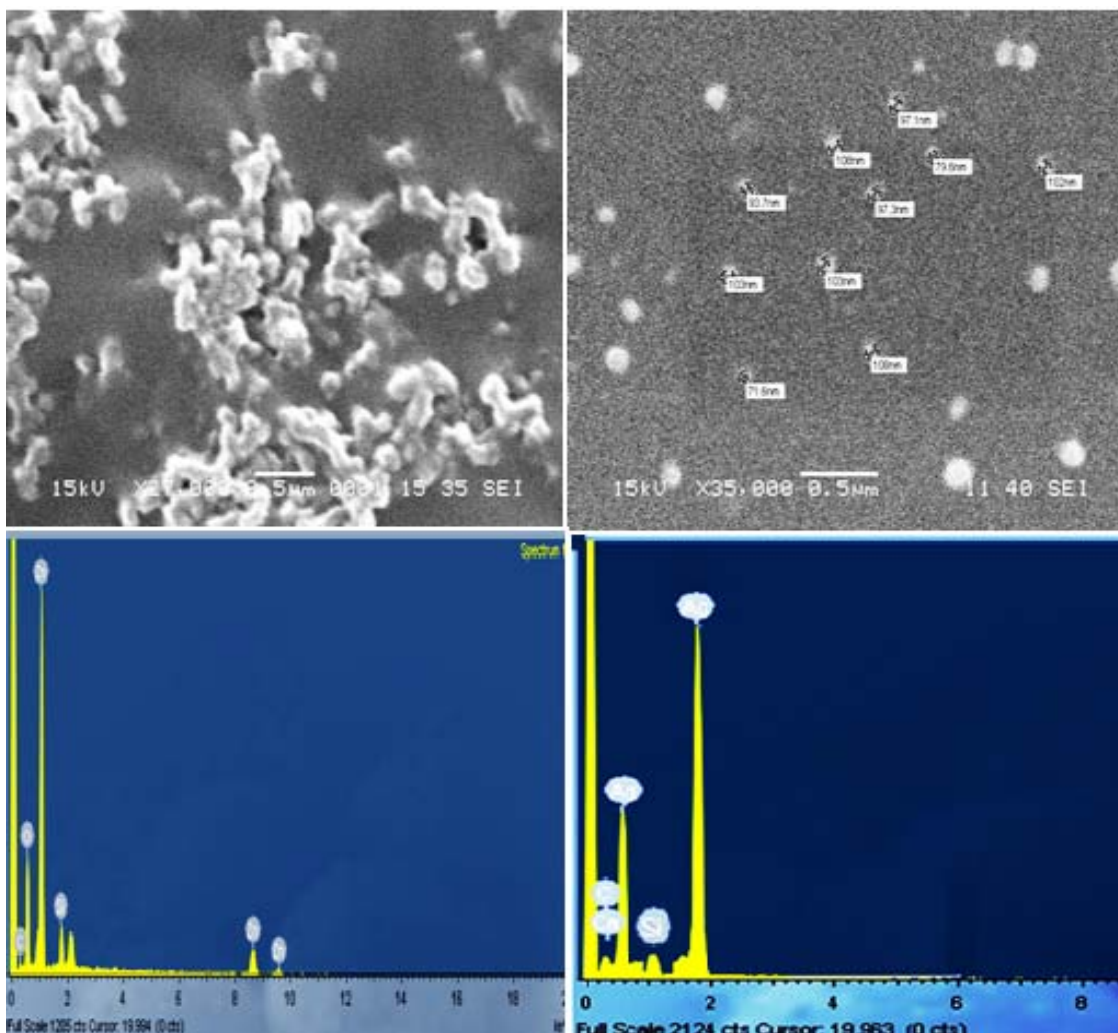


Figure 7. SEM micrograph of ZnO and Ag nanoparticles synthesized by chemical reduction method and green synthesis process.

4.2.5 Dynamic light scattering particle size analyzer

The Figure 8(a) shows the particle size of the ZnO and Ag nanoparticles samples. After analyzing data, it was found that ZnO nanoparticle size were in the range of 80-120nm. Similarly Figure 8(b) shows the graphical representation of average particle size distribution of Ag nanoparticles. They were in a range

of 20-140 nm. However, beyond 100 nm range the percentage of nanoparticles present is very less.

The highest fraction of Ag NP present in the solution was of 50nm.

From the plot it was evident that the solution was consist of nanoparticles having various sizes which are indeed in agreement of the result obtained by SEM analysis.

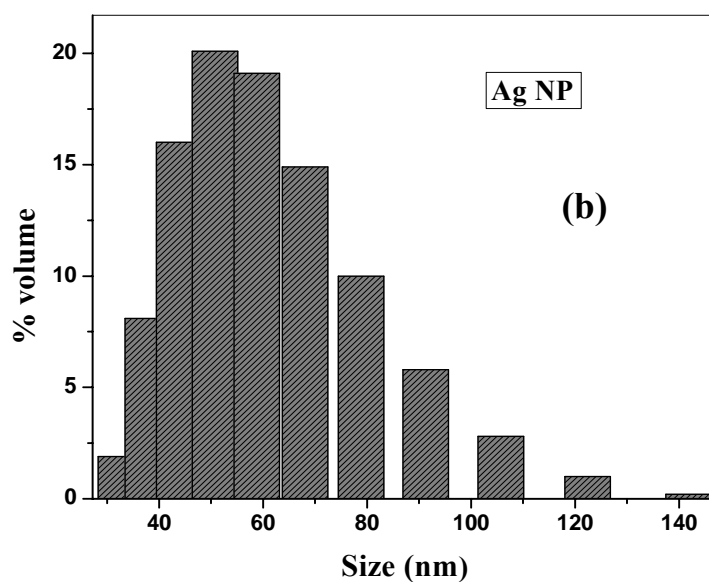
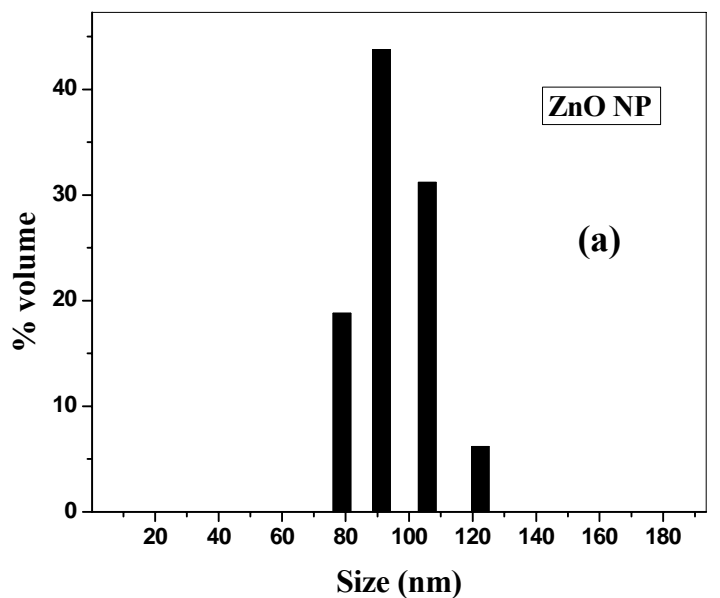


Figure 8. Particle size distribution of (a) ZnO and (b) Ag nanoparticles synthesized by chemical reduction method and green synthesis process.

4.2.6 Thermo gravimetric analysis (TGA) of ZnO sample

TGA or thermogravimetric analysis ZnO NP was carried out to observe characteristic weight loss with temperature. The TGA analysis of synthesized nano ZnO was shown in Figure 9. The synthesized nano ZnO is subjected to a heating from room temperature to highly thermal temperature of 1000°C. The initial weight loss took place at around a temperature of 180°C. The bulk ZnO did not show any weight loss when heated up to 1000°C but in case of soluble starch a weight loss at around 312°C was observed, which is matching the results reported in (Vigneswaran et al., 2006) equal to the degradation temperature of starch. These properties helped to characterize and confirm the formation of ZnO nanoparticles (range obtained from 90-100nm).

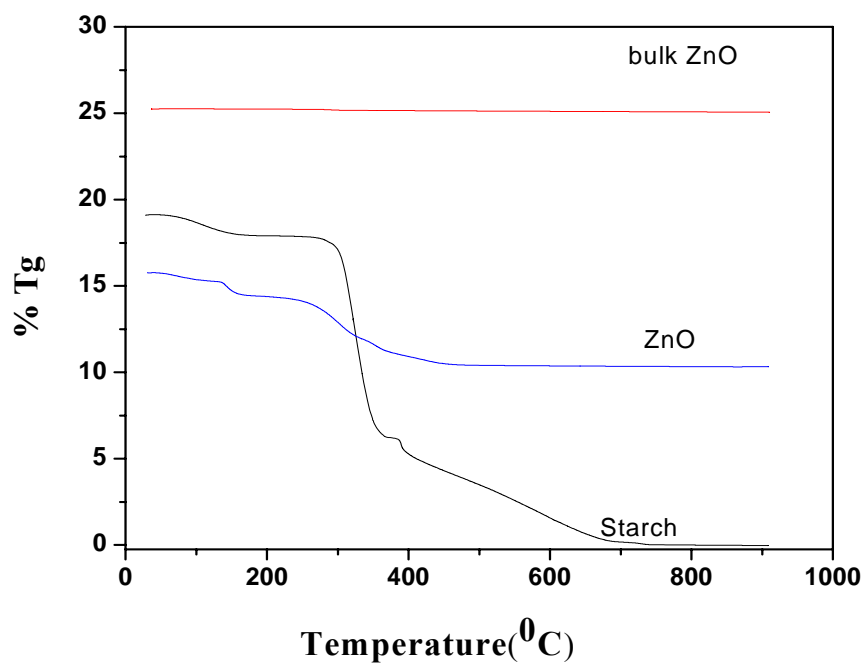


Figure 9. Thermo gravimetric analysis of bulk ZnO (red), nano-ZnO (blue) and soluble starch (black).

4.3 Antibacterial Assays:

ZnO and Ag nanoparticles bactericidal effect was studied against four different pathogenic bacteria *E.coli*, *Bacillus subtilis*, *Pseudomonas aeruginosa*, *Streptococcus pneumonia*. These nanoparticles were dispersed in autoclaved Millipore water by ultrasonication. Aqueous dispersion of ZnO and Ag nanoparticles of desired concentration was made.

4.3.1 Disc Diffusion test of ZnO and Ag nanoparticles

The effect of different concentration of ZnO NP like-5mM, 10mM, 15mM and 0.2mM, 0.3mM and 0.6mM of silver nanoparticles on bacteria was performed. As shown in Figure 10 as we increased the concentration of ZnO nanoparticles the antibacterial activity of ZnO nanoparticles increased. Figure 10 shows a clear inhibition zone treated with ZnO nanoparticles whereas the standard antibiotics like vencomycin, erythromycin, and tobramycin shows smaller zone of inhibition as compared to the nanoparticles treated discs. Also Figure 11 shows a clear inhibition zone treated with Ag nanoparticles whereas the standard antibiotics like vencomycin, erythromycin shows smaller zone of inhibition as compared to the nanoparticles treated discs.

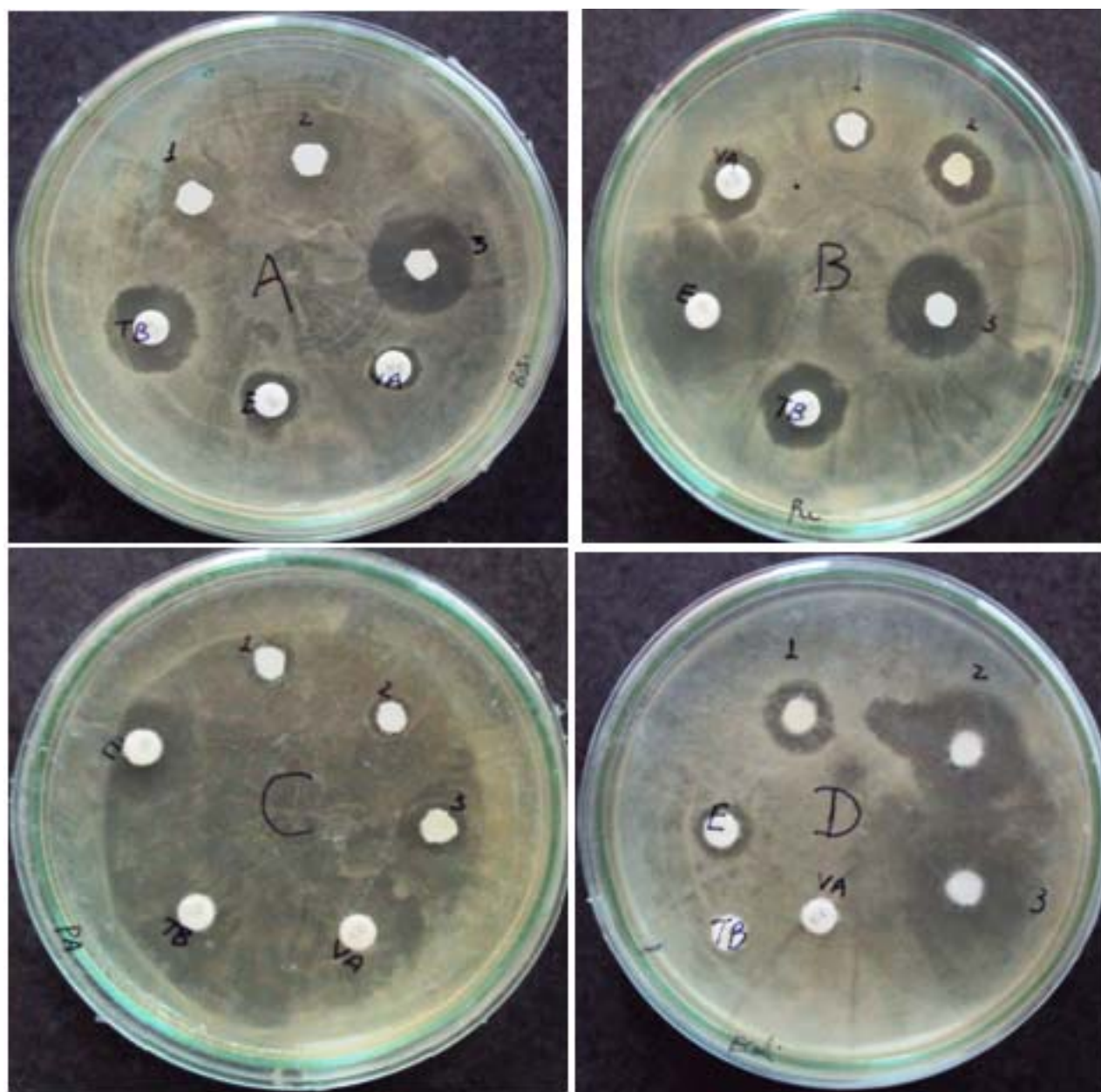


Figure 10. Images of antibacterial activities of discs of different concentration of ZnO nanoparticles (5mM, 10mM and 15mM) and other antibiotics on (A) *Bacillus subtilis* (B) *Streptococcus pneumoniae* (C) *Pseudomonas aeruginosa* (D) *E.coli* (N=nanoparticles, VA= Vancomycin, E= Erythromycin, TB = Tobramycin).

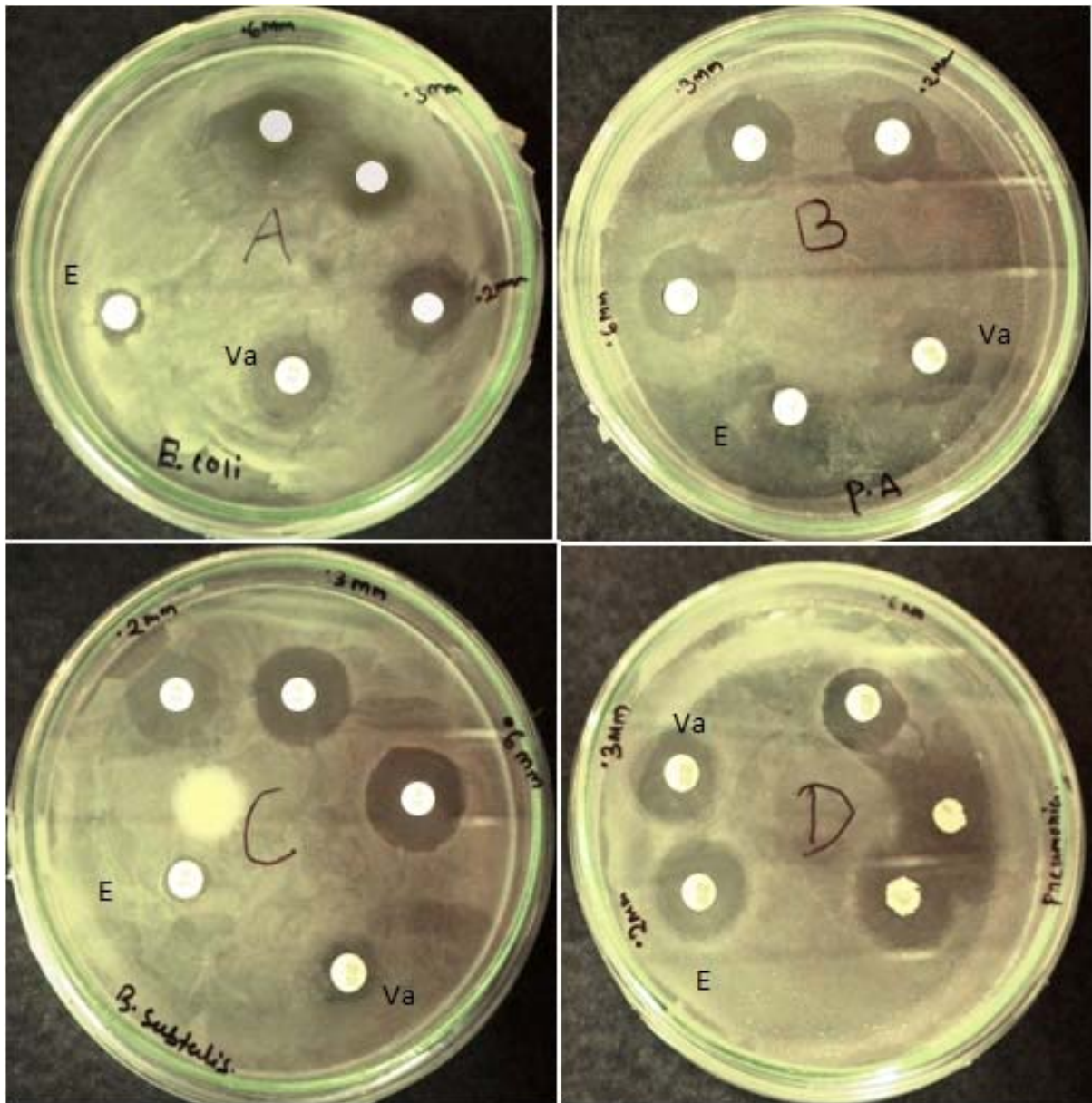


Figure 11. Images of antibacterial activities of discs of different concentration of Ag nanoparticles (0.2mM,0.3mM and 0.6mM) and other antibiotics on A. *E coli* B. *Pseudomonas aeruginosa* C. *Bacillus subtilis* D. *Streptococcus pneumonia* (N=nanoparticles, VA= Vancomycin, E= Erythromycin).

Table 1. Zone of Inhibition of Antibacterial test of ZnO NP

Bioactive agent		Zone of inhibition (Diameter, cm)			
		<i>E.coli</i>	<i>Bacillus subtilis</i>	<i>Pseudomonas aeruginosa</i>	<i>Streptococcus pneumonia</i>
ZnO nanoparticle	5 mM	3.2	2.2	nil	0.2
	10 mM	4.7	4.1	nil	3.1
	15 mM	4.8	4.8	3.1	4.9
Erythromycin(10mcg/disc)		0.8	0.7	0.6	4.8
Vancomycin(10mcg/disc)		nil	nil	nil	0.6
Tobramycin(10mcg/disc)		nil	3.1	nil	3.2

Table 2. Zone of Inhibition of Antibacterial Test of Ag NP

Bioactive agent		Zone of inhibition (Diameter, cm)			
		<i>E.coli</i>	<i>Bacillus subtilis</i>	<i>Pseudomonas aeruginosa</i>	<i>Streptococcus pneumonia</i>
Ag nanoparticle	0.2 mM	2.5	3.2	3.1	3.2
	0.3 mM	3.4	4.2	3.3	3.4
	0.6 mM	4.2	4.3	4.2	3.8
Erythromycin(10mcg/disc)		nil	nil	0.6	4.1
Vancomycin(10mcg/disc)		0.8	nil	0.8	3.8

4.3.2 Antimicrobial test by the estimation of Colony Forming Units (CFU)

Figure 12 shows the plot of number of bacterial colonies grown on nutrient agar plates as a function of concentration of ZnO/Ag nanoparticles. The numbers of CFU have been observed to reduce significantly with the increasing ZnO/Ag nanoparticles loading.

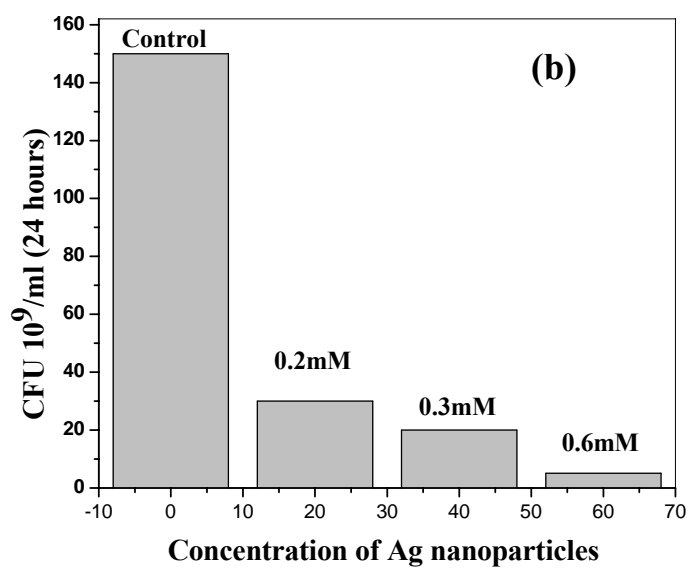
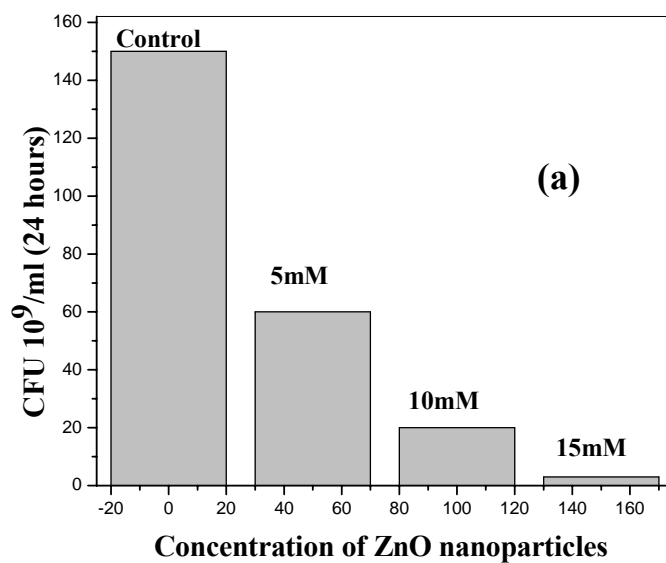


Figure.12. Antimicrobial characterization by CFU as a function of (a) ZnO and (b) Ag nanoparticles concentration on agar plates.

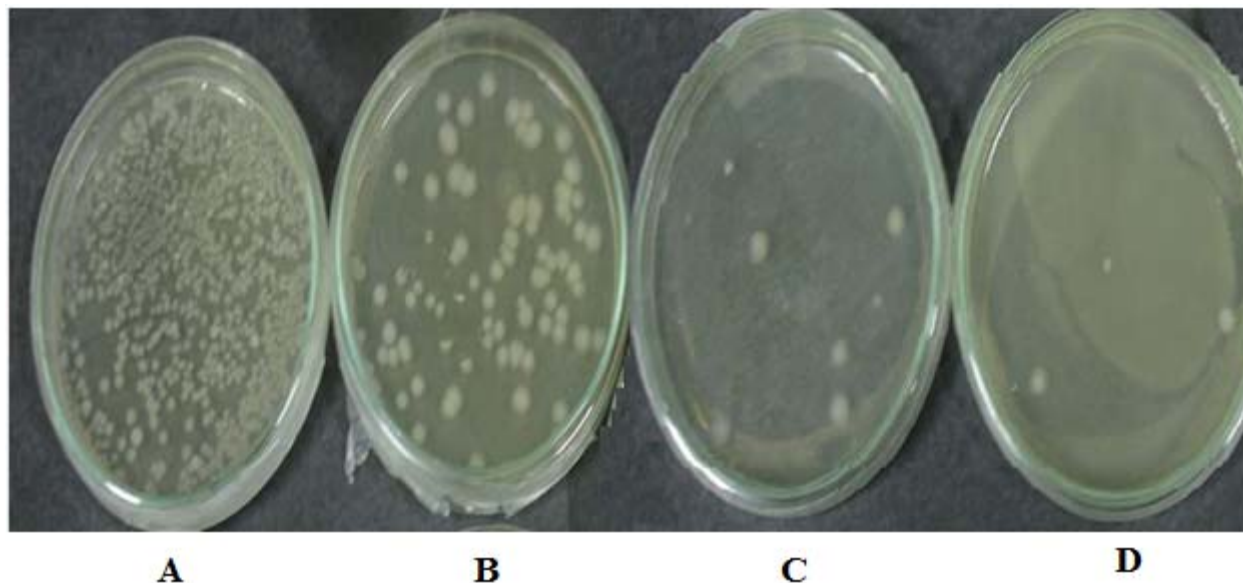


Figure 13. Digital photograph of *E. coli* colonies grown on nutrient agar plate as a function of silver nanoparticle concentration. A) Control B) 0.2mM C) 0.3mM D) 0.6mM silver NP concentration.

4.3.3 Growth kinetics study

The synthesized ZnO and Ag nanoparticles were administered to *E.coli* with various concentrations to investigate the growth behavior. From the Figure 14 it was noticed when the concentration of ZnO and Ag were increased the growth was reduced. This clearly indicates that NP produced toxicity to *E.coli* and therefore the growth was inhibited. 15mM ZnO and 0.6mM Ag NP concentration was found to have highest toxicity to the bacteria.

Also specific growth rate, μ was calculated in each case and presented in the tabular form in table-3.

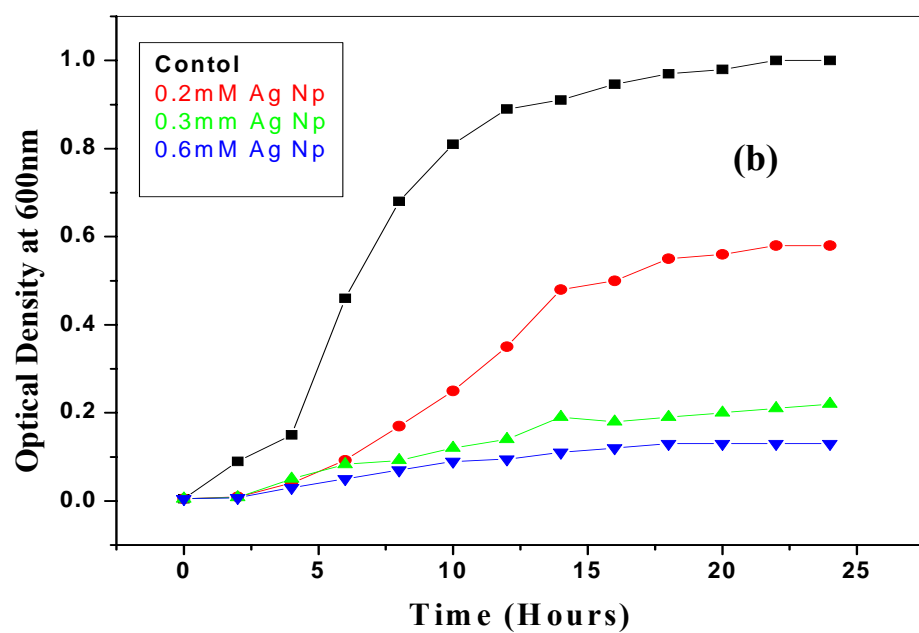
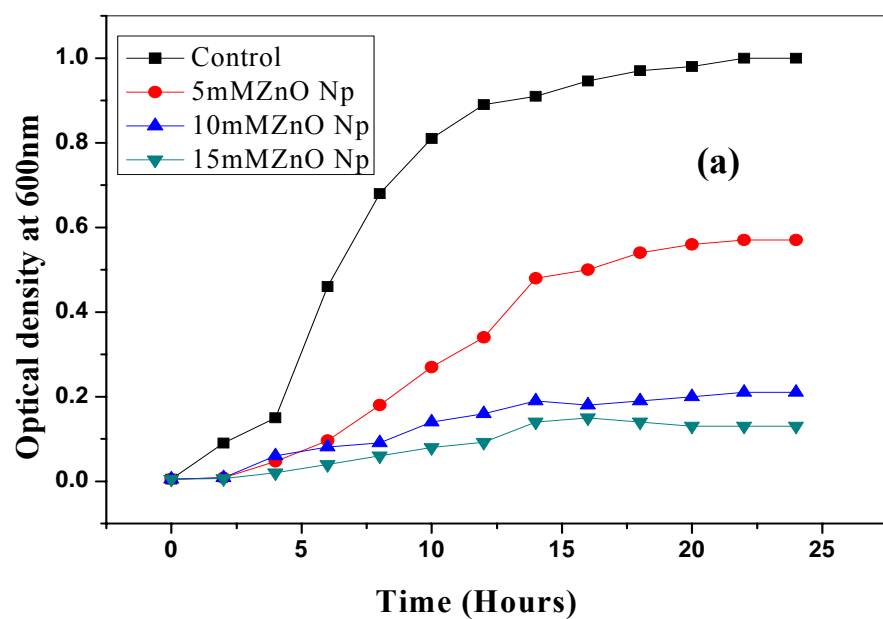


Figure 14. The effect of (a) ZnO and (b) Ag nanoparticles on the growth of *E.Coli*.

Table 3. Calculation of specific growth rate of *E.coli* in the presence of ZnO and Ag NP

NP concentration (mM)	Specific Growth rate (h⁻¹)
0	0.21
5	0.14
10	0.05
15	0.02
NP concentration (mM)	Specific Growth rate (h⁻¹)
0	0.21
0.2	0.16
0.3	0.07
0.6	0.04

4.4 Effect of ZnO and Ag nanoparticles in the genetic expression level of β -glucosidase *in vivo*

β -glucosidase was expressed in *E.coli* and its biological activity was monitored using the protocol mentioned in Material and Methods section no-3.8.1. The culture was incubated with various concentrations of ZnO and Ag nanoparticles and the biological activity of the expressed β -glucosidase

was measured. The activity unit presented absorbance (A) and this was plotted against ZnO/Ag NP concentration which is shown in Figure 15 and Figure 16.

It was observed from the plot that with the increase of NP concentrations, the biological activity of β -glucosidase was enhanced substantially *in vivo* and beyond 15 mM and 0.5 mM concentration of ZnO and Ag NP, respectively, there was no further change of activity.

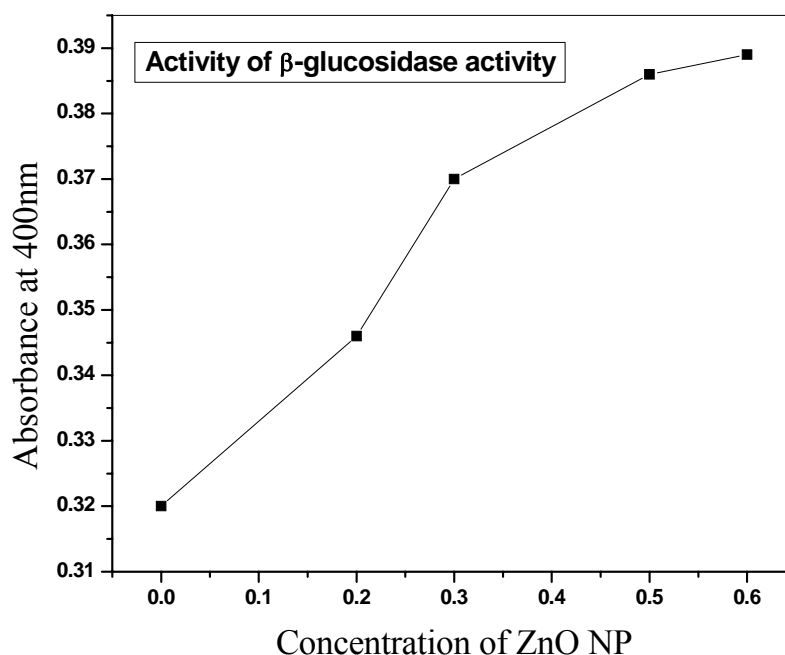


Figure 15. The effect of β -glucosidase activity with ZnO nanoparticles treated with *E.coli* strain.

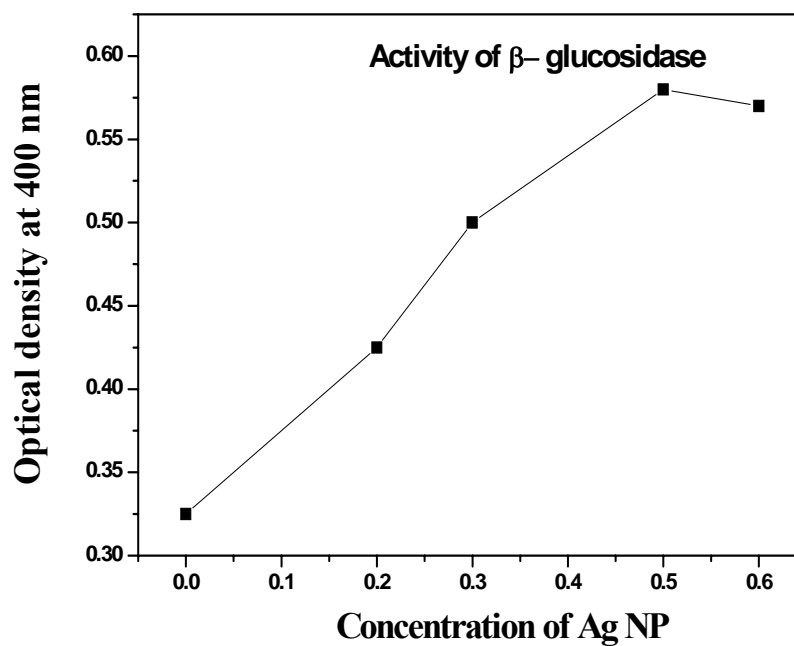


Figure 16. Activity of β -glucosidase activity with Ag nanoparticle treated *E.coli* strain.

In the presence of enzyme β -glucosidase, the substrate p-nitrophenyl- β -glucoside (PNPG) is converted into the products p-nitrophenol (PNP) and glucose. This reaction was monitored by the change in color from colorless to pale yellow colored solution shown in Figure 17.

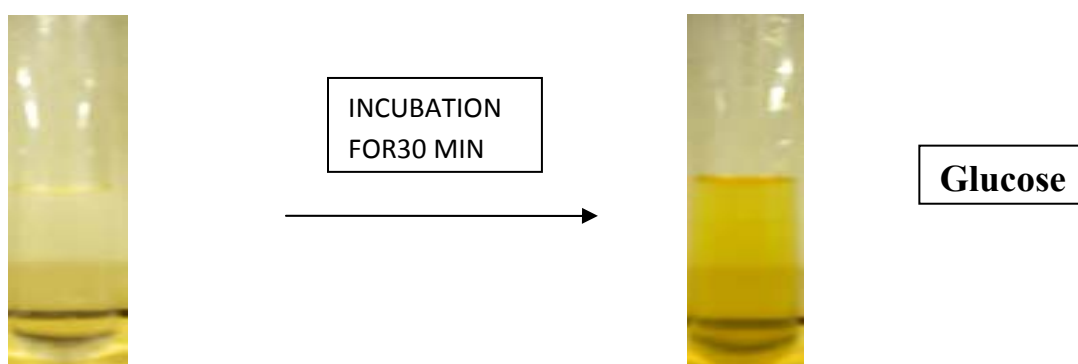


Figure 17. Conversion of PNPG to PNP and glucose

4.5 Formation of conjugate between α -lactalbumin and ZnO nanoparticles

From the DLS particle size distribution (106-164nm) of protein NP conjugate, it was evident that multiple number of protein molecules interacted with nanoparticles. Based on the size distribution data given in Table-4, following probable mechanism might be possible.

Possible mechanisms:

1. All proteins present in the solution are associated in conjugate formation with nanoparticles.
2. One NP interacted with various number of protein molecules with minimum number of 27 and maximum number of 85.
3. Protein upon binding with NP might was triggered to form aggregates.
4. If the case-3 was true, then a heterogeneous conjugates were formed.

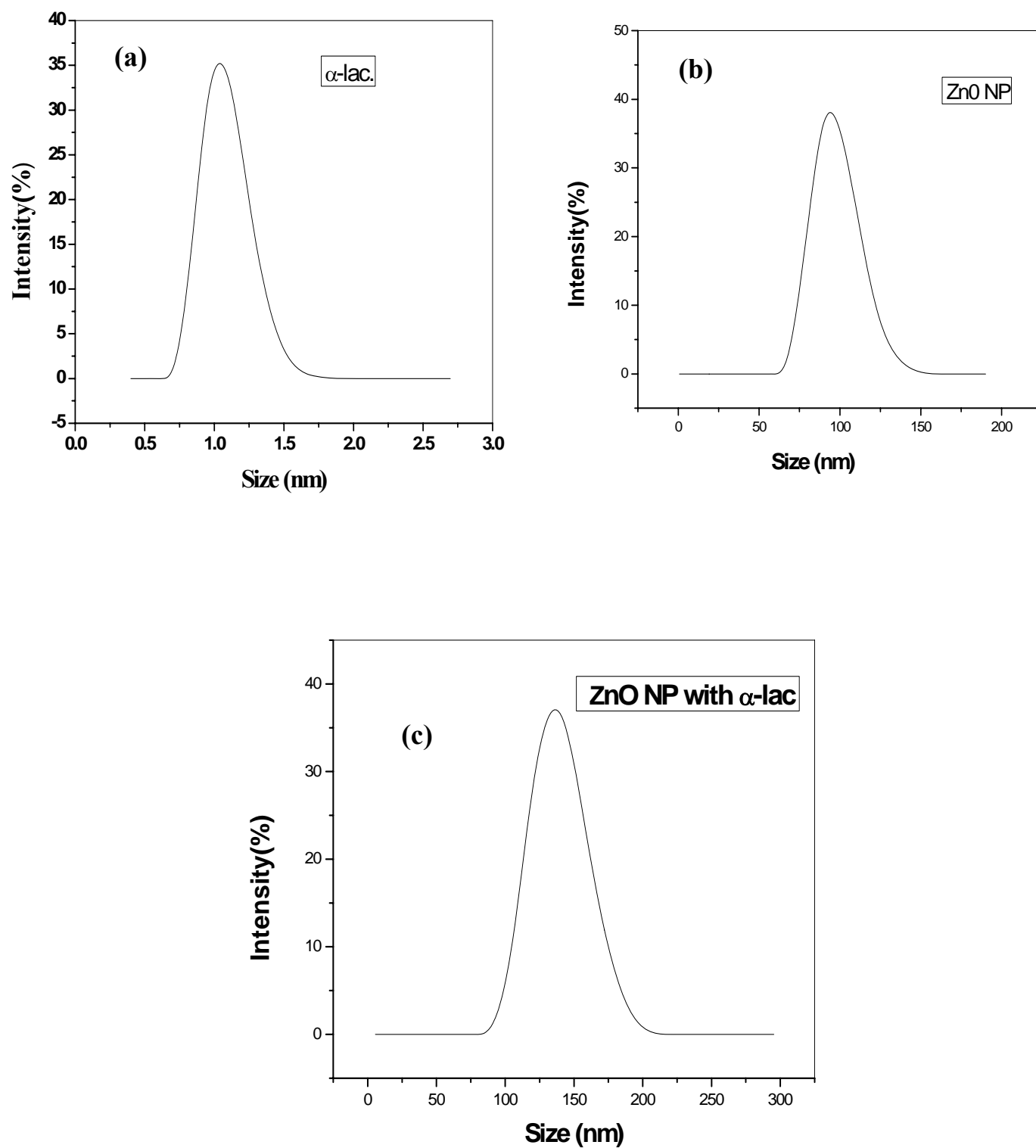
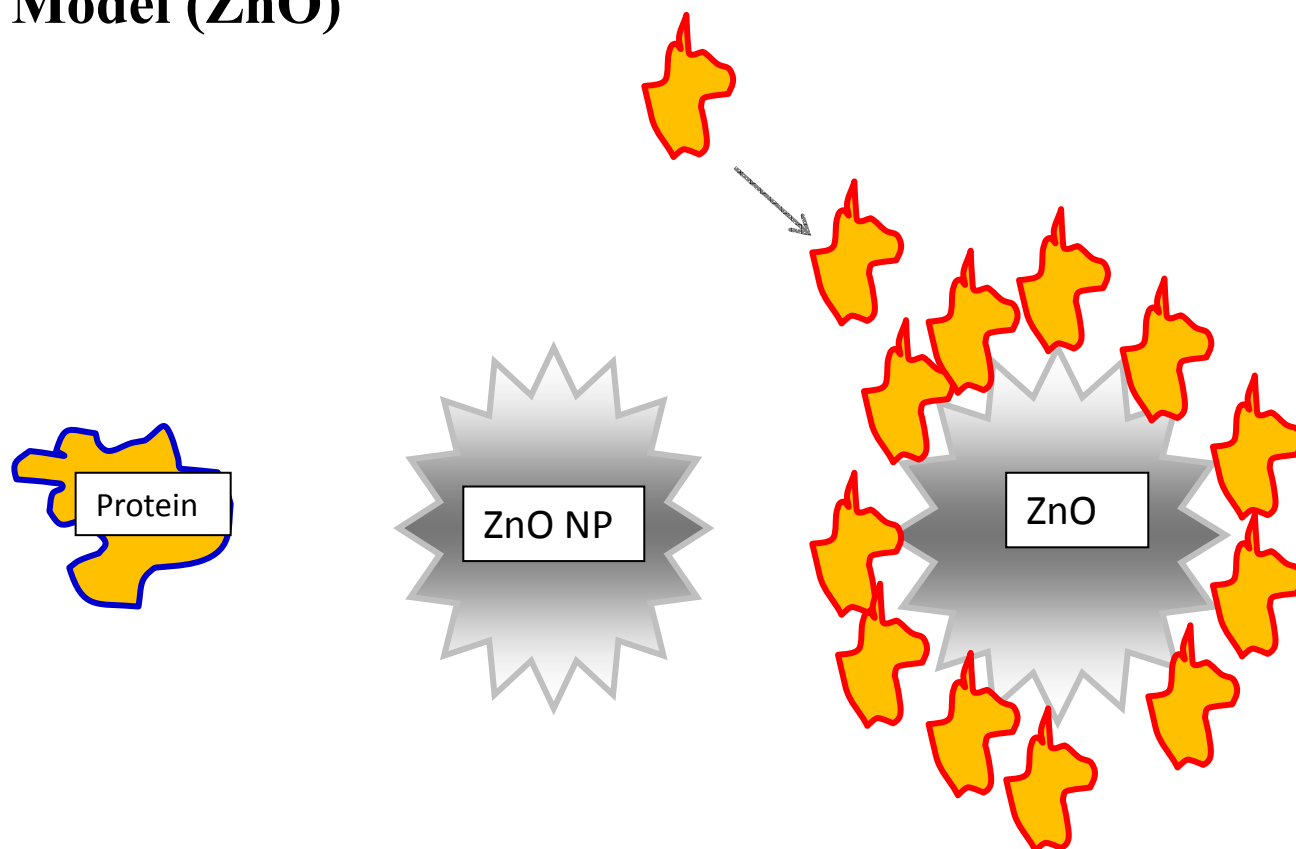


Figure 18. Formation of conjugate between α -lactalbumin and ZnO nanoparticles monitored by DLS particle size analyzer.(a) pure α -lactalbumin, (b) ZnO NP (c) ZnO NP with α -lactalbumin.

Table 4 Size distribution and average size of protein, ZnO and conjugate.

Protein distribution range	Avg. protein dia.	ZnO distribution range	Avg. ZnO range	Conjugate distribution range	Avg. Conjugate dia.
0.75-1.5 nm	1 nm	79-122 nm	91 nm	106-164 nm	142 nm

Model (ZnO)



Proposed Model of α -lactalbumin protein and ZnO nanoparticles interaction *in vitro*.

4.6 Formation of conjugate between α -lactalbumin and Ag nanoparticles

Similarly in case of Ag nanoparticles, it was clear that in the protein NP (Ag) interaction, multiple protein molecules interacted with nanoparticles. Based on the data (Table-5) the following mechanism can be predicted.

Possible mechanisms:

1. All protein molecules in the test sample solution are associated in conjugate formation with nanoparticles.
2. One NP interacts with various no. of protein molecules with a minimum number of 57 and maximum no. of 262
3. Protein on binding with NP might have been triggered to form aggregates
4. Therefore there might be a chance of having heterogeneous mixture (size) of conjugates.

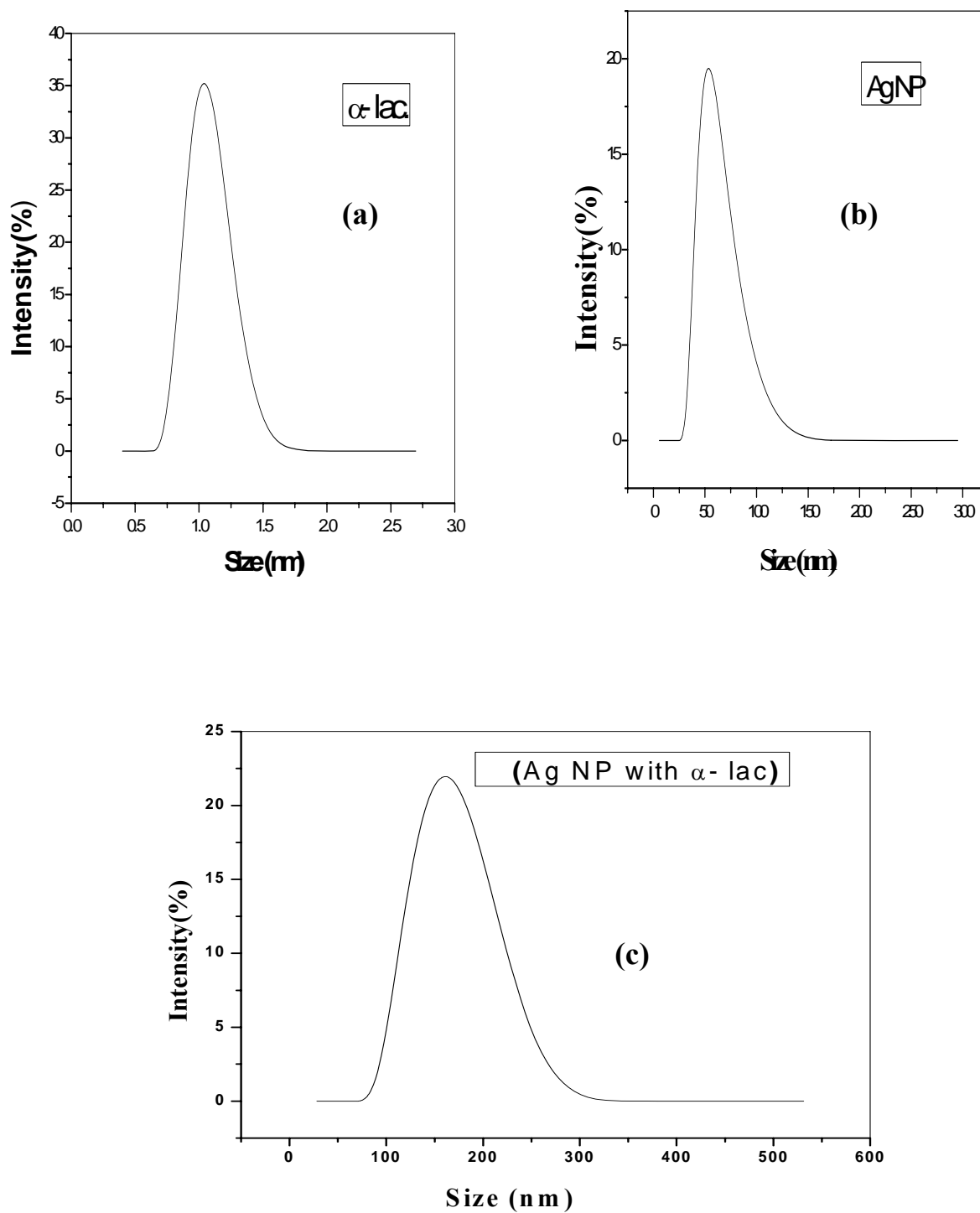
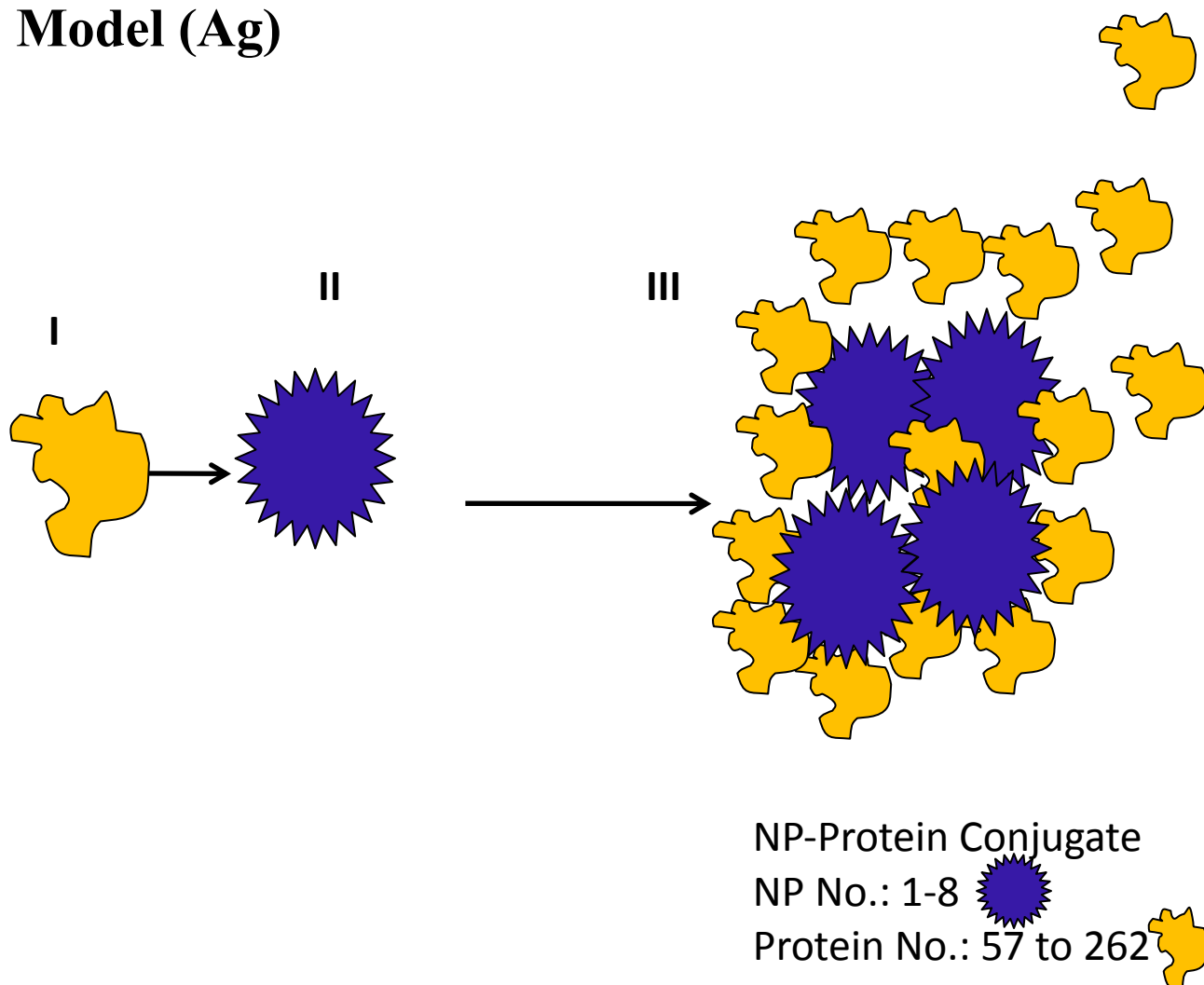


Figure 19. Formation of α -lactalbumin and Ag nanoparticles conjugate *in vitro*, monitored by DLS particle size distribution. (a) Pure α -lactalbumin, (b) Ag NP (c) Ag NP with α -lactalbumin.

Table 5 Size distribution and average size of protein, Ag and conjugate.

Protein distribution range	Avg. protein distribution	Ag distribution range	Avg. Ag range	Conjugate distribution range	Avg. Conjugate dia.
0.75-1.5 nm	1 nm	33-122 nm	50 nm	91-295nm	165 nm

Model (Ag)



Proposed Model of α -lactalbumin protein and Ag nanoparticles interaction *in vitro*.

4.7 *In vitro* interaction of green synthesized Ag nanoparticle and bovine α -lactalbumin monitored by spectroscopic techniques

4.7.1 Fluorescence emission spectra measurement

The tryptophan fluorescence emission spectra of bovine α -lactalbumin in free solution and in the presence of nanoparticles were monitored within the spectral region between 300 and 400 nm. The fluorescence emission measurements were recorded using excitation maxima of 280 nm.

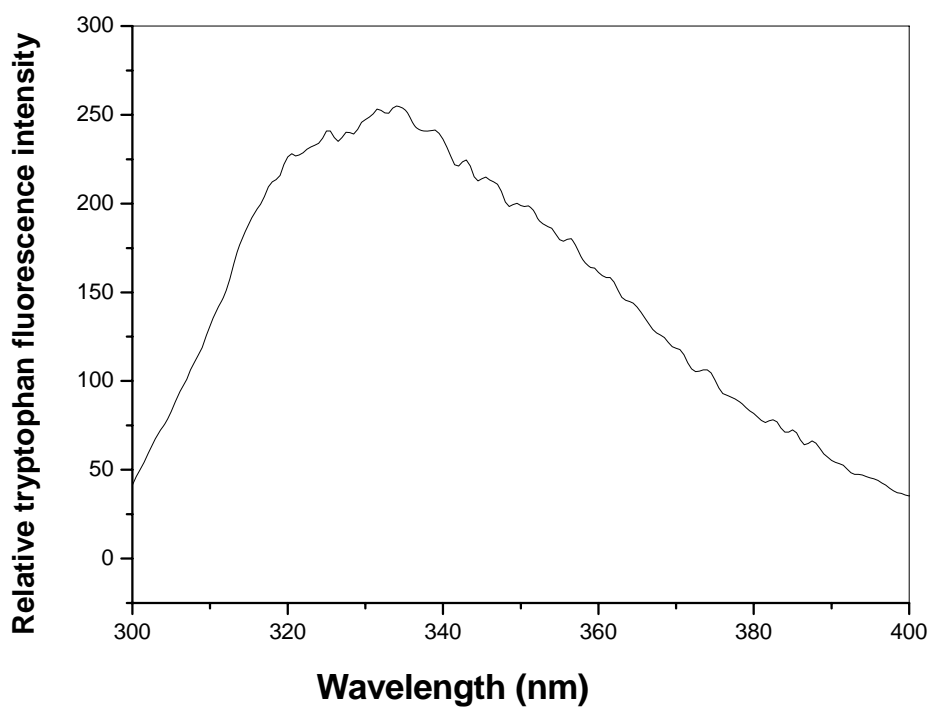


Figure 20. Intrinsic fluorescence spectrum of 0.2mg/ml bovine α -lactalbumin in 20 mM sodium phosphate buffer, pH 7.0. Emission spectrum was measured at 25°C in the wavelength range of

300- 400 nm at the $\lambda_{\text{max}}^{\text{Ex}}$ 280 nm. The excitation and emission band passes were 5 nm and 7.5 nm, respectively for excitation and emission and the scan rate was 60 nm/min.

In the Figure 21 it was shown that in presence of nanoparticles the tryptophan fluorescence intensity was reduced substantially. NP, after binding with protein molecule, brings down the fluorescence intensity of tryptophan of the protein indicated a havoc conformational change of the protein. This also revealed that on binding, the tryptophan molecules are transferred to a more polar environment or they were exposed to the NP solutions which basically act as quencher shown in Figure 21. When all acryl amide was added, the trp fluorescence was quenched drastically, indicated tryptophan were on the surface or crevice which were accessible to the quencher. When NP was added in a solution of protein and acryl amide mixture, very little quenching was observed that was contributed by acryl amide, revealed that tryptophan molecules were already quenched by NP particles and probably trp were in the protein-NP binding site. (Figure 22)

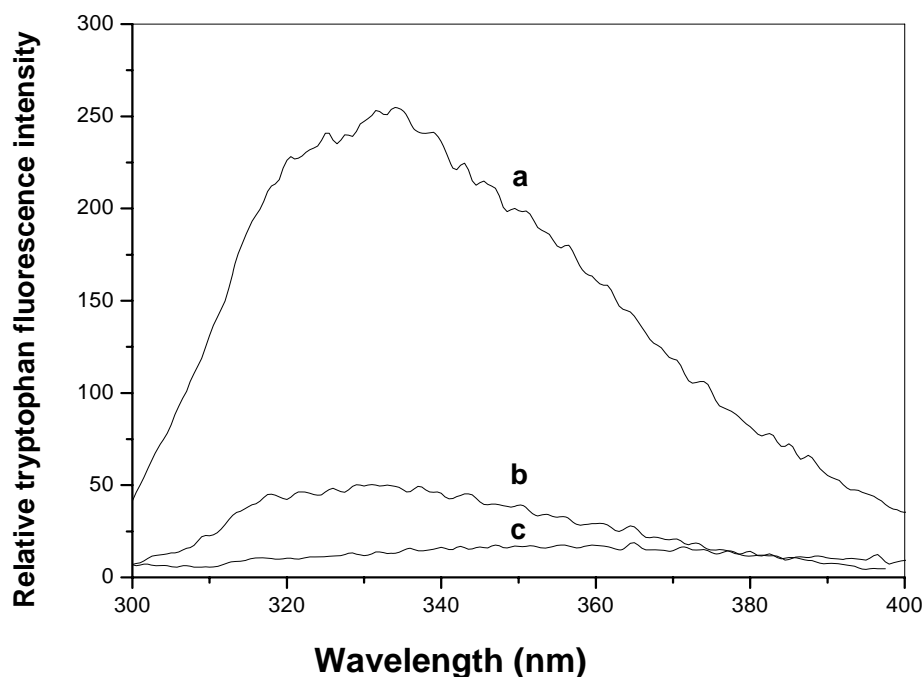


Figure 21. Emission fluorescence spectrum of (a) pure α -lactalbumin (0.2mg/ml), (b) α -lactalbumin-AgNP complex and (c) pure Ag nanoparticle (50 μ g/ml). The protein was excited at 280 nm.

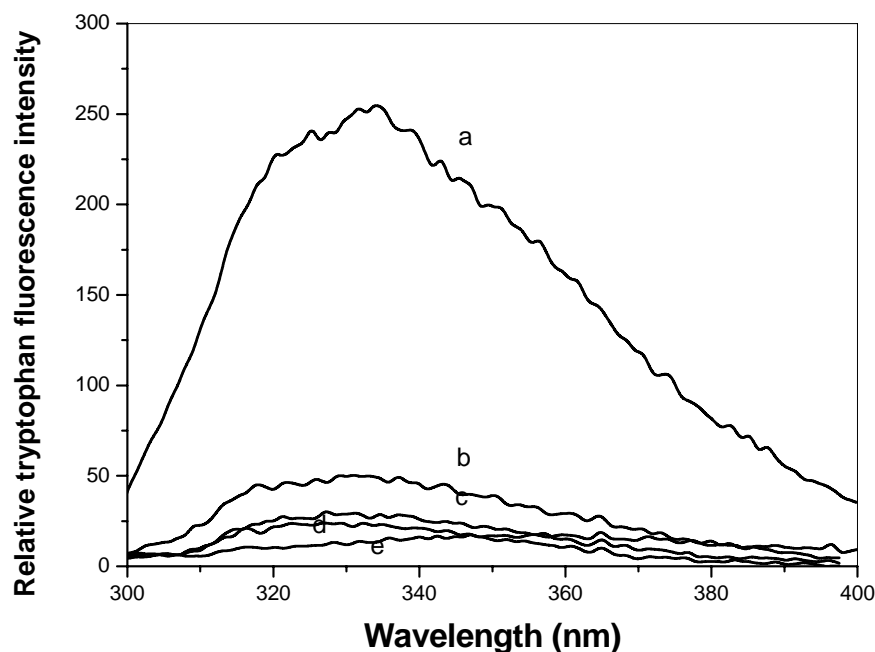


Figure 22. Emission Fluorescence spectrum of pure (a) α -lactalbumin (0.2mg/ml) (b) pure protein in the presence of 200 mM acrylamide (c) Pure Ag nanoparticle (50 μ g/ml), and (d) α -lactalbumin-NP complex, (e) α -lactalbumin-NP conjugate in presence of 200 mM acrylamide. The trp was excited at 280 nm and emission spectrum was recorded.

4.7.2 Far-UV CD measurement

Far-UV CD spectra of the solution of bovine α -lactalbumin and various concentration of Ag NP were measured. Appropriate control values were subtracted. The CD signal in mdegree and wavelength was plotted in Figure 23. When NP was added the protein solution for 30minutes, the CD ellipticity signal

of the protein was reduced, indicated the destruction of secondary structural components of the protein like α -helix, β -sheets and random coil (RC), which indirectly means the drastic structural change of the protein. The protein that was α -helix dominant in its native state and had no β -sheets, upon interaction with NP, gains significant amount of β -sheets components at the cost of RC and β -turn. The produced conformation of the protein having good amount of β -sheets content might have converted the protein to an aggregation-prone one.

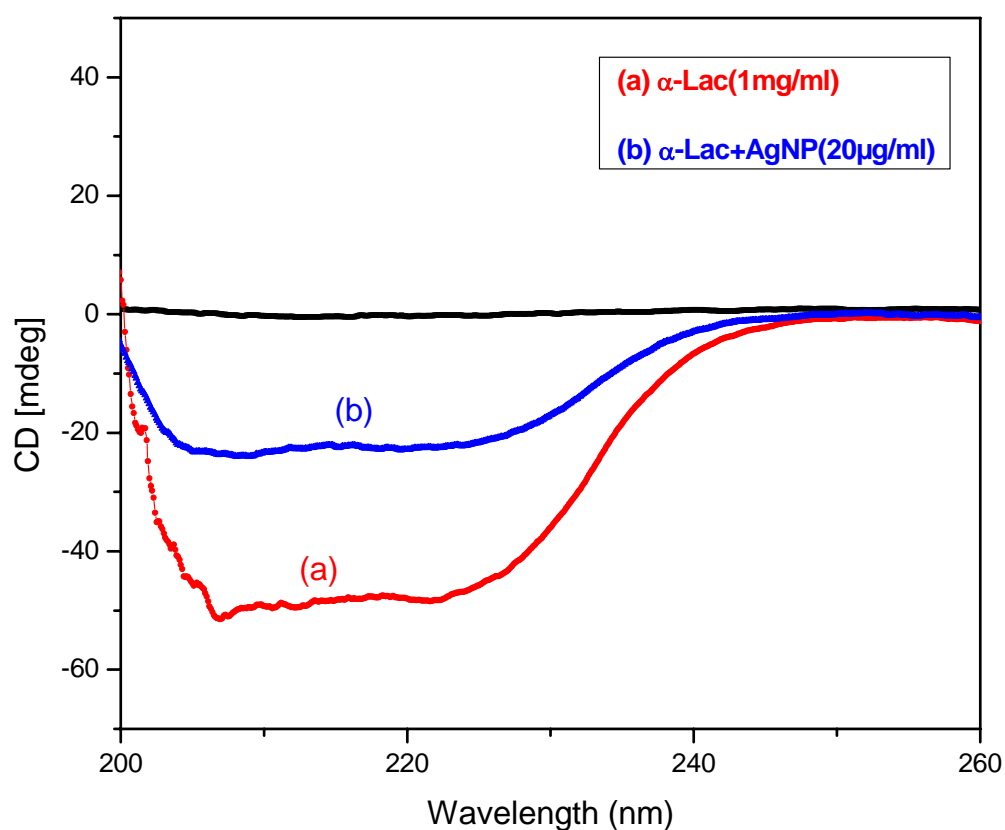


Figure 23. CD spectrum of (a) Pure α -lactalbumin (b) protein NP complex.

The data from each spectrum was analysed using online k2D software to get percentage secondary structural components like α -helix, β -sheet, β -turn and random coil which is shown in the Table 6.

Table 6. Secondary Structure estimation of pure α -lactalbumin protein and α -lac –Ag NPs complex by Circular Dichroism.

Secondary Structural Components	α -Lac (1mg/ml)		α -Lac + AgNPs (20 μ g/ml)	
	Fraction Ratio		Fraction Ratio	
α -Helix	0.2	27.2 %	0.2	26.4 %
β -sheet	0.0	0.0 %	0.1	13.8 %
β -Turn	0.2	29.7 %	0.2	21.8 %
Random coil	0.4	43.1 %	0.3	38.0 %
Total	1	100 %	1	100 %

From the Table 6, it was clear that the protein in its native form (pure solution) had no β -sheets. So it is a protein of α -helix dominant. When NP interacts with protein, its structure (3D) must have changed largely which was also reflected from the data of percentage β -sheets. Although there was a little decrease of α -helix, the increase of β -sheet percentage was huge (from 0% to 14%). This was happened at the cost of β -turn and random coil when their percentage was reduced.

The production of β -sheets in the protein's secondary structure not only provides rigidity of the structure but it also makes the protein more aggregation protein.

CHAPTER-5

CONCLUSION

AND

FUTURE PROSPECTS

The conclusion drawn from the present investigations are as follows:

1. ZnO and Ag nanoparticles were synthesized successfully by chemical reduction and green synthesis methods (From *Citrus sinensis*), respectively.
2. The detail characterization of the nanoparticles was carried out using UV-Vis spectroscopy, Dynamic Light Scattering (DLS) particle size analysis, Scanning Electron Microscopy (SEM), X-Ray Diffraction (XRD) analysis. From Dynamic Light Scattering (DLS) particle size and SEM image analysis, the average particle size was found to be 90 nm and 50 nm, respectively for ZnO and Ag.
3. Antibacterial potential of both ZnO and Ag nanoparticles as a function of nanoparticles concentration was tested against four different bacteria like *Escherichia coli*, *Pseudomonas aeruginosa*, *Bacillus subtilis*, and *Streptococcus pneumonia*. The test was performed by both Disc diffusion assay and colony forming unit (CFU) estimation method. From the study, both types of nanoparticles were observed to have strong antimicrobial potential. When the result was compared with the effect by antibiotics like Vencomycin, Tobramycin and Erythromycin, nanoparticles were found more potent than antibiotics.
4. The growth study of *Escherichia coli* was carried out in presence of different concentration of both nanoparticles to observe the effect on the growth of the bacteria in liquid media. It was observed that both the nanoparticles strongly affected the specific growth rate of *E.coli*. It was also observed that the growth rate was strongly inhibited by the presence of small concentration of nanoparticles.

5. *In vivo* biological activity of expressed β -glucosidase enzyme in *Escherichia coli* was measured in the presence of various concentrations of ZnO and silver nanoparticles. It was found that the incubation of *Escherichia coli* in the presence of nanoparticles caused the substantial enhancement of the biological activity of β -glucosidase *in vivo*.
6. *In vitro* interaction between α -lactalbumin and both nanoparticles were also investigated. When the binding experiments were monitored in DLS particle size analyzer, the stable protein-NP conjugate formation was confirmed. The result also helped to develop a model where multiple numbers of proteins bind to a single or multiple NP molecules.
7. The interaction between α -lactalbumin protein and nanoparticles were also studied by tryptophan fluorescence and circular dichroism spectroscopic techniques. The tryptophan fluorescence measurement of the protein revealed the fact that the protein undergoes a havoc structural change while interacting with NP. The tryptophan fluorescence quenching study revealed that tryptophan residues are possibly in the binding site.
8. Circular dichroism spectroscopic measurement confirmed the change of secondary structure of the protein in the presence of NP. Although there was no β -sheet in the native protein, binding with NP cause the formation of substantial amount of β -sheet in the protein's secondary structure.

The present research work leaves the following future prospects:

- Anti-fungal and anti-cancerous activity of the ZnO and Ag nanoparticles may be investigated in details.
- Various plants and fruit extract can be used to synthesize Ag nanoparticles to find a more non-toxic and economical method of synthesis.
- Detail mechanistic study of antibacterial function of nanoparticle may be elucidated.
- Study the detail mechanism how nanoparticle enhances the *in vivo* expression of β -glucosidase.
- Nanoparticles may be used to examine the effect on other industrially and clinically important gene expression *in vivo*.
- α -lactalbumin and nanoparticles conjugate may be applied in various cancer cell to observe any anti-cancerous potential of the protein-NP conjugate.

CHAPTER- 6

REFERENCES

Albrecht, M.A., Evans, C.W. and Raston, C.L. (2006). Green chemistry and the health implications of nanoparticles. *Green Chem.* 8, 417-420.

Andrade, M.A., P. Chacón, J.J. Merelo and F. Morán. 1993. Evaluation of secondary structure of proteins from UV circular dichroism using an unsupervised learning neural network. *Prot. Eng.* 6, 383-390.

Ahmad, A., Mukherjee, P., Senapati, S., Mandal, D., Khan, M. I., Kumar and R., Sastry, M. (2003). Extracellular biosynthesis of silver nanoparticles using the fungus *Fusarium oxysporum*. *Colloids Surf B Biointerf.* 28, 313–318.

Asharani, P.V., Toxicity of silver nanoparticles in zebrafish models. (2008). *Nanotechnology* 19, 255102.

Barber D. J. and Freestone, I. C. (1990). An investigation of the origin of the color of the *Lycurgus cup* by analytical transmission electron microscopy. *Archaeometry.* 32, 33-45.

Baker, C., and Pradhan, A. (2004). Synthesis and antibacterial properties of silver nanoparticles. *Journal of Nanoscience and Nanotechnology.* 5, 287–293.

Fratini, A., Pellegrini, N., Nicastro, D. and Sanctis O. (2005). First-principles study of the adsorption of NH_3 on Ag surfaces. *Mater Chem Phys.* 94, 148-152.

Gardea-Torresdey, J. L., Gomez, E., Peralta-Videa, J. R., Parsons, J. G., Troiani, H and Jose-Yacaman, M. (2003). Alfalfa sprouts: a natural source for the synthesis of silver nanoparticles". *Langmuir*, 19, 1357–1361.

Henglein,A., (1999). Formation of Colloidal Silver Nanoparticles: Capping Action of Citrate.J. *Phys. Chem. B.* (1999). *103*, 9533-9539.

Husseiny, M. I., Abd El-Aziz, M., Badr, Y and Mahmoud, M. A. (2007). Biosynthesis of gold nanoparticles using *Pseudomonas aeruginosa*. *Spectrochim. Acta A.* *67*. 1003–1006.

Henglein, A. (1989). Small-particle research: physicochemical properties of extremely small colloidal metal and semiconductor particles. *Chem. Rev.* *89*, 1861-1864.

Hahn H. (1997). Unique Features and Properties of Nanostructured Materials. *Nanostructured Materials.* *9*, 3.

Jose, R. M., Jose, L. E and Alejandra. C. (2005). The bactericidal effect of silver nanoparticles. *Nanotechnology.* *16*, 2346–2353.

Jana, N. R., Sau, T. K., and Pal., T. (1999). Growing Small Silver Particle as Redox Catalyst. J. *Phys.Chem.* 103-115.

Jones .N, Ray.B and Manna.C. (2007).Antibacterial activity of ZnO nanoparticle suspension on a broad spectrum of microorganisms. *Fems microbiol* *279*(1), 71-6.

Jain. D, Daima. H. K,Kuchhwaha. S, and Kothari S.L.,(2009).Plant mediated silver nanoparticles using papaya fruit extract and evaluation of their antimicrobial activities.Digest journal of nanomaterials and biostructures. *4*, 557-563.

Koziara, J. M., Lockman, P. R., Allen, D. D. and Mumper, R. J. (2003). In situ blood-brain barrier transport of nanoparticles. *Pharm. Res*, 20, 1772.

Lomolino, G., Zocca, F., Spettoli, P., and Lante, A. (2006). Detection of β -d Glucosidase and Esterase Activities in Wild Yeast in a Distillery Environment. *The Institute of Brewing & Distilling*. Vol. 112, No. 2.

Lovley, D. R., Stolz, J. F. and Nord, G. L. (1987). Anaerobic production of magnetite by a dissimilatory iron-reducing microorganism. *Nature*, 330, 252-254.

Lee, P. C. and Meisel, D., (1982). Adsorption and Surface Enhanced Raman of Dyes on Silver and Gold Sols. *J. Phys. Chem.* 86, 3391.

Limbach, L. K., Wick, P., Manser, P., Grass, R. N., Bruinink, and Stark, W. J. (2007). Catalytic activity on oxidative stress. *Environmental Science Technology*. 41, 4158.

Li, S.; Shen, Y.; Xie, A.; Yu, X.; Qiu, L.; Zhang, and L.; Zhang, Q. (2007). “Green synthesis of silver nanoparticles using Capsicum annum L. extract”. *Green Chemistry*, 9, 852–858.

Look D.C, (2001). Recent advances in ZnO materials and devices. *mat sci eng*; B.80 383.

Moore, A., and Goettmann, F., (2006). The plasmon band in noble metal nanoparticles an introduction to theory and applications. *New Journal of Chemistry*. 30, 1121-1132.

Morones, J. R. and Elechigerra, J. I. (2005). Interaction of silver nanoparticles with HIV-1. *Nanotechnology*, 16, 2346.

Merelo, J.J., M.A. Andrade, A. Prieto and F. Morán. 1994. Proteinotopic Feature Maps. *Neurocomputing*. 6, 443-454.

Nair, B. and Pradeep, T. (2002). Coalescence of nanoclusters and formation of submicron crystallites assisted by Lactobacillus strains. *Crystal Growth Design*. 2, 293–298.

Nagy, A. and Mestl, G. (1999). High temperature partial oxidation reactions over silver catalysts. *Appl Catal A*. 188,337.

Nair.S., Sasidharan. A, Nair .S, and Raina.S. (2008). Role of size scale of ZnO nanoparticles on toxicity toward bacteria and osteoblast cells. *J.Mater sci*.20, S235-S241.

Oberdorster, G., Sharp, Z., Atudorei, V., Elder, A., Gelein, R..and Kreyling, W. (2004). Translocation of inhaled ultrafine particles to the brain. *Inhal Toxicology*. 16,437-440.

Permyakova , E.A. and Berlinerb, L.J. (2000). α -Lactalbumin: structure and function. *FEBS*.473, 269-274.

Pfeil, W. (1998). Is the Molten Globule a Third Thermodynamic State of Protein. The Example of α -Lactalbumin. *Proteins Structure, Function and Genetics* . 30, 43–48.

Roe, D., Karandikar, B., Bonn-Savage, N., Gibbins, B. and Roullet, J. B. (2008). Antimicrobial surface functionalization of plastic catheters by silver nanoparticles. *Journal of Antimicrobial Chemotherapy*. 61, 869–76.

Rosi, N. L. and Mirkin, C.A. (2005). Nanostructures in Biodiagnostics. *Chemical Review*. 105,1547.

Ramboarina, S. and Redfield, C. (2003). Structural Characterisation of the Human α -Lactalbumin Molten Globule at High Temperature. *J. Mol. Biol.* 330, 1177–1188.

Shankar, S.S., Rai, A., Ahmad, A. and Sastry, M., (2004). Rapid synthesis of Au, Ag and bimetallic Au core Ag shell nanoparticles using Neem (*Azadirachta indica*) leaf broth. *J. Colloid Interface Science*. 275, 496–502.

Shankar, S. S., Ahmad, A. and Sastry, M. (2003). Geranium leaf assisted biosynthesis of silver nanoparticles. *Biotechnology Prog.* 19,1627–1631.

Shankar, S. S., Rai, A., Ahmad, A. and Sastry, M. (2004). Rapid synthesis of Au, Ag, and bimetallic Au core-Ag shell nanoparticles using Neem (*Azadirachta indica*) leaf broth. *J. Colloid Interface Science*. 275,496–502.

Shankar, S. S., Ahmad, A., and Sastry M. (2003). Geranium leaf assisted biosynthesis of silver nanoparticles, *Biotechnol. Prog.* 19, 1627-1635.

Shrivastava, S., Bera, T., Roy, A., Singh, G., Ramachandrarao, P. and Dash, D. (2007). Characterization of enhanced antibacterial effects of novel silver nanoparticles. *Nanotechnology*. 18,9.

Shibata, S., Aoki, K., Yano, T. and Yamane, M., (1998). *Journal of SOL-gel Science and Technology*. 11,279-286.

Solomon, S.D., Bahadory, M., Jeyarajasingam, A.V., Rutkowsky, S.A. and Boritz, C. (2007). Synthesis and Study of Silver Nanoparticles. *Journal of Chemical Education*. Vol.84, No.2. 322-325.

Suber, L., Sondi, I., Matijevic, E. and Goia, D.V. (2005). Preparation and the mechanisms of formation of silver particles of different morphologies in homogeneous solutions. *Center for Advanced Materials Processing, Clarkson University, Potsdam. NY. 13699-5814, USA*.

Shang, L., Wang, Y., Jiang, J., and Dong, S. (2007). PH-Dependent Protein Conformational Changes in Albumin Gold Nanoparticle Bioconjugates. A Spectroscopic Study. *Langmuir*. 23, 2714-2721.

Shang W., Joseph H., Jonathan S. and Richard W. (2007). Unfolding of ribonuclease A on silica Nanoparticles surface. *nanoletters* 7, No.7 1991-1995.

Svensson, M., Håkansson, A., Mossberg A.K., Linse, S. and Svanborg, C. (2000). Conversion of α -lactalbumin to a protein inducing apoptosis. *PNAS*. 97, 4221–4226.

Tien, D.C., Liao, C.Y., Huang, J.C., Tseng K.H., Lung, J.K., Tsung, T.T., Kao, W.S., Tsai, T.H., Cheng, T.W., Yu, B.S., Lin, H.M. and Stobinski, L. (2008). Novel technique for preparing a nano-silver water suspension by the arc-discharge method. *Rev. Adv. Mater. Sci.* 18. (2008). 750-756.

Tessier, P. M., Velev, O. D., Kalambur, A. T., Rabolt, J. F., Lenhoff, A. M. and Kaler, E. W. (2000). Assembly of gold nanostructured films templated by colloidal crystals and use in surface-enhanced Raman spectroscopy. *J. American Chemical Society*. 122, 9554.

Vigneshwaran, N., Ashtaputre, N. M., Varadarajan, P. V., Nachane, R. P., Paralikar, K. M. and Balasubramanya, R. H. (2007). Biological synthesis of silver nanoparticles using the fungus *Aspergillus flavus*. *Material Letter*. 61, 1413–1418.

Vigneshwaran, N., Nachane, R.P., Balasubramanya, R.H. and Varadarajan, P.V. (2006). A novel one-pot ‘green’ synthesis of stable silver nanoparticles using soluble starch. *Carbohydrate Research* 341, (2006). 2012–2018.

Vigneshwaran,N., Kumar.S., Varadarajan,P.V. and Prasad.V. (2006).Functional finishing of cotton fabrics using Zinc oxide soluble starch nano composites.*Nanotechnology* 17,5087-5095.

Willner I., Baron R.. and Willner B. (2006). Growing metal nanoparticles by enzymes. *Advance Material*. 18, 1109–1120.

Whitmore.L,Sokal.A,and Richard.C,(2001).Surface structure of Zinc oxide (10_10) using anatomistic,semi-in.nite treatment.

Xia Y. and Halas, N. J. (2005). Shape-controlled synthesis and surface plasmonic properties of metallic nanostructures. *MRS Bulletin*. 30,338-343.

Xi, T., Kovochich, M., Brant, J., Hotze, M., Sempf, J.and Oberley, T. (2006). *Nano Letter*, 6,1794.

Yin, B., Ma, H.,Wang,S. and Chen,S. (2003). Electrochemical Synthesis of Silver Nanoparticles under Protection of Poly(*N*-vinylpyrrolidone). *J. Phys. Chem. B*,(2003). 107, 8898-8904.

Yang, J.T., Wu, C.-S.C. & Martinez, H.M. (1986). Calculation of protein conformation from circular dichroism. *Methods Enzymol*. 130, 208–255. 136

Zhang.L, Jiang.Y, Povey.M, and York.D.,(2007).Investigation into the antimicrobial behavior of suspension of ZnO nanoparticles(ZnO nanofluids).*Journal of Nanoparticles Research*,9, 479-489.

Zeng, F., Hou, C., Wu, S. Z., Liu, X. X., Tong, Z., and Yu, S. N. (2007). Silver nanoparticles directly formed on natural macroporous matrix and their anti-microbial activities. *Nanotechnology*. 18, 1–8.

Zhou, Y., Yu, S. H., Cui, X. P., Wang, C. Y. and Chen, Z. Y. (1999). Formation of Silver Nanowires by a Novel Solid–Liquid Phase Arc Discharge Method. *Chem. Mater.* 11, 545–546.

Zeng, D.W., Xie.C.S. and Zhu B.L,2003. Synthesis and characterstics of Sb-doped ZnO *material science and Engineering*,B 10,468-72.

Zhu.B.L,Zeng D.W and Song W.L (2005). Investigation of gas sensitivity of Sb-doped ZnO nanoparticles,material chemistry and physics,89,148-153.